

Electricity Price Prediction Using Multi-Kernel Gaussian Process Regression combined with Kernel-Based Support Vector Regression

Abhinav Das¹, Stephan Schlüter², and Lorenz Schneider³

¹Faculty of Mathematics and Economics, Ulm University

²Institute of Energy Engineering and Energy Economics, Ulm University of Applied Sciences

³Emlyon Business School, Lyon, France

Abstract

This paper presents a new hybrid model for predicting German electricity prices. The algorithm is based on the combination of Gaussian Process Regression (GPR) and Support Vector Regression (SVR). Although GPR is a competent model for learning the stochastic pattern within the data and interpolation, its performance for out-of-sample data is not very promising. By choosing a suitable data-dependent covariance function, we can enhance the performance of GPR for the tested German hourly power prices. However, since the out-of-sample prediction depends on the training data, the prediction is vulnerable to noise and outliers. To overcome this issue, a separate prediction is made using SVR, which applies margin-based optimization, having an advantage in dealing with non-linear processes and outliers, since only certain necessary points (support vectors) in the training data are responsible for regression. The individual predictions are then combined using the performance-based weight assignment method. A test on historic German power prices shows that this approach outperforms its chosen benchmarks such as the auto-regressive exogenous model, the naive approach, as well as the long short-term memory approach of prediction.

1 Introduction

The prediction of energy prices, particularly electricity prices, has been a challenging yet compelling research problem since the liberalization of European electricity markets. Electricity differs from other energy commodities, such as oil or gas, due to several reasons such as non-storability and – lately – weather dependency. Modeling features such as hourly electricity prices, supply/demand, and production has become more and more difficult with an increasing share of renewable power in total energy production [1]. The volatility of the market has increased significantly due to the dependence on weather conditions that are intermittent in nature [2]. There are many other factors which make price prediction more complicated, such as non-stationarity of the data, complex interdependencies, temporal correlations etc. Comparatively accurate electricity price prediction is highly desired by various stakeholders including consumers, production utilities, and policy makers [3, 4]. On the one hand, constructing a model that efficiently incorporates complex factors and provides relatively accurate predictions often comes with high computational costs due to the model’s complexity. On the other hand, simplifying the model to reduce computational demands can lead to a loss in prediction accuracy. Therefore, the challenge is to develop a balanced model that is both simple and interpretable, yet still provides sufficiently accurate predictions. Achieving this balance is a key task in model development.

In the German market, the share of renewable energy is significantly higher than in other markets, such as the French one. For example, aggregated for 2023 the share was above 50% [5]. As a consequence hourly day ahead prices are more volatile due to variable weather conditions. To model such a

Keywords: Electricity price prediction, Gaussian Process, Support Vector Regression
MSC: 62-07, 62M20

volatile commodity, several approaches such as statistical/probabilistic methods [6, 7], machine learning/deep learning methods [8, 9], or their combination (typically known as hybrid approach [10, 11]) are employed. Given the challenges, a prediction method which is relatively simple and explainable, and can model inter-relationship between the price and its influencing factors in an efficient way becomes indispensable. To construct such a balanced model we have formulated a prediction model which is a linear combination of the Gaussian Process Regression (GPR) and the Support Vector Machine (SVR). GPR is a probabilistic approach and SVR is a machine learning approach. Both are kernel-based methods which are very good at capturing the non-linear relationship between the commodities and their influencing factors. We have analyzed various kernel functions for both GPR and SVR that fit the characteristics of the German Electricity price data. GPR gives the uncertainty associated to the predicted values, whereas the SVR makes point forecasts. Hence, we used the conformal prediction approach for the interval associated to the point forecast via SVR. The implementation of the proposed combined model is carried out using the German electricity price data, the predicted residual load data, and the total renewable energy production data for the years 2021, 2022, and 2023 individually. To analyze the performance of the proposed approach, we compared the predictions of our combined model with the Autoregressive Exogenous (ARX) model, the Long Short-term Memory (LSTM) model, and the Naive approach. The comparison confirms that the proposed model outperforms the aforementioned benchmark models.

The remainder of the paper is organized as follows. In Section 2, we give a brief overview of the related work in this field of research. In Section 3, the electricity price data and factors that affect the prices are described, as well as our data sources and the arrangement of the data. A brief introduction to Gaussian processes is given in Section 4, in which a detailed formulation for the GPR and the covariance functions is also discussed. Section 5 focuses both on the deployment of kernel-based SVR to predict electricity prices, as well as the prediction interval for SVR. In Section 6, we introduce the so-called hybrid model as the weighted sum of the predicted prices using SVR and GPR. In Section 7, we test our hybrid model against chosen benchmarks. We conclude our work and future prospects of this research in Section 8. Additional mathematical reasoning and explanations are given in the Appendix.

2 Related Work

The prediction of electricity prices has gained considerable importance since the liberalization of European power markets. Approaches such as the auto-regressive integrated moving average (ARIMA) model or its extension, the seasonal auto-regressive integrated moving average (SARIMA) model, have been widely applied to forecast electricity prices. In [12], the ARIMA model has been used to predict the electricity prices of Spain and California; the model performed with non-uniformity in both of the markets. Similarly, in [13], the authors proposed a hybrid ARIMA model combined with wavelet transform for short-term electricity price forecasting focusing on the Spanish electricity market. Their results demonstrated the effectiveness of the hybrid model in capturing both short-term fluctuations and long-term trends in electricity prices. A similar study [14] combined ARIMA with an artificial neural network (ANN) to forecast electricity prices in the western region of Denmark, in which they showed the superiority of ARIMA over the seasonal naive model. In [15], the authors explored the combination of machine learning algorithms, including SVMs, ANNs, and decision trees, for electricity price forecasting. Their study showed that ensemble methods combining multiple algorithms often outperform individual models, leading to more accurate predictions. In recent years, deep learning techniques have gained traction in electricity price prediction. For instance, [3] proposed a fuzzy neural network for short-term electricity price forecasting. By incorporating fuzzy logic into neural networks, their model improved prediction accuracy, particularly in capturing uncertainty and non-linearity in electricity price data. Furthermore, in [16] the use of convolutional neural networks (CNN) for daily electricity price forecasting is investigated. Their study demonstrated the ability of CNNs to extract non-linear features from historical price data, leading to enhanced prediction performance compared to traditional models. In [17], the authors have compared the use of long short-term neural networks (LSTM) and CNNs with a SARIMA model. In [18] different methods are tested for better prediction using different regularizations. In [19], the authors have used the LASSO-based auto-regression method for the prediction the electricity prices. In addition to data-driven approaches, stochastic models have also been employed for electricity price prediction.

Despite the progress made in electricity price prediction, several challenges remain. One is the increasing complexity of the electricity market, characterized by the integration of renewable energy

sources and the increasing number of electric vehicles and batteries. These developments introduce additional uncertainty and non-linearity into price data, requiring more sophisticated modeling techniques. In addition, the deregulation of electricity markets has led to increased market volatility and unpredictability, which poses challenges to traditional forecasting methods. As a result, there is a growing need for innovative approaches that can adapt to changing market dynamics and provide reliable predictions in uncertain environments. In conclusion, electricity price prediction is a multifaceted problem that requires a combination of mathematical, statistical, and computational techniques. Although significant progress has been made in this field, ongoing research is needed to address emerging challenges and develop more robust and accurate forecasting models. While time series models like ARIMA, and SARIMA provide a strong foundation for understanding temporal patterns, the limitation lies in their assumption of linear relationships, which restricts their ability to capture complex non-linear dependencies in time series data [20]. There are approaches like generalized auto-regressive conditional heteroskedasticity (GARCH) and threshold auto-regressive (TAR), which deal with the non-linearity within the data sets, however, these models still fall short in terms of overall flexibility and handling high-frequency data. Machine learning and deep learning techniques offer flexibility and scalability for capturing complex relationships in data, but require large amounts of data to generalize well and are prone to overfitting when applied to noisy, sparse, or volatile data, such as hourly time series [21]. GPR and SVR offer a robust solution by being non-parametric models that are inherently capable of handling both linear and non-linear relationships. GPR, with its probabilistic framework, can model uncertainty and capture both short-term and long-term dependencies through flexible kernel functions [22]. SVR, with its kernel-based approach, excels at handling high-dimensional data and is highly robust to outliers and noise [23]. The combination of these two methods, through an ensemble approach, allows for better generalization in high-frequency time series data, making them a superior choice over traditional time series models and deep learning techniques, especially when the dataset is noisy, sparse, or irregular.

3 Electricity Data

In 2023, 57% of the total load in Germany was provided by renewable sources, with the (onshore) wind being the dominant technology followed by solar and hydropower [5]. This considerable share combined with its stochastic nature motivates us to consider renewable sources as one fundamental driver for electricity prices in Germany. For our analysis, we are using the data provided by the Federal Network Agency of Germany (German: Bundesnetzagentur, Website). The data includes historic prices, residual load forecast, and total renewable energy production forecast. As a general practice in the electricity market, electricity produced via renewable sources is traded with guarantee, and hence gross demand minus the hourly production via renewable sources, which is called “*residual load*” becomes more relevant as it determines the amount of additional energy needed to be supplied by the non-renewable source of energy. The higher residual load reflects that the generation of energy from renewable sources is low and non-renewable sources are required to satisfy demand [24]. Giving information about residual load and total electricity produced by renewable sources explicitly to the model helps the algorithm to learn underlying price patterns. As shown in Figures (1)-(3) the data display certain levels of heteroscedasticity, noise, and extreme values, which affect the modeling. A log transformation of the data and normalization help to smooth such properties.

Weather data is not considered, even though they are relevant, since weather is local and station-based. However, we deal with aggregated data here. The problem is not about the availability of the data, but about how to integrate it into our model in an efficient way. In addition, a large number of features are also demanding from a data quality point of view. Eventually, weather does not directly affect electricity prices, but only indirectly through renewable energy production. The latter is considered in our model through solar, wind, biomass, and hydropower. In this paper, we have arranged the datasets as follows: We consider data with an hourly resolution for the electricity price, the forecasted residual load, and the forecasted total renewable energy (day ahead), which means that for one day we have 24 data points for each variable. We stack each day in a single vector for each variable, which will be a time series of the price, load, and energy production indexed by hours of days

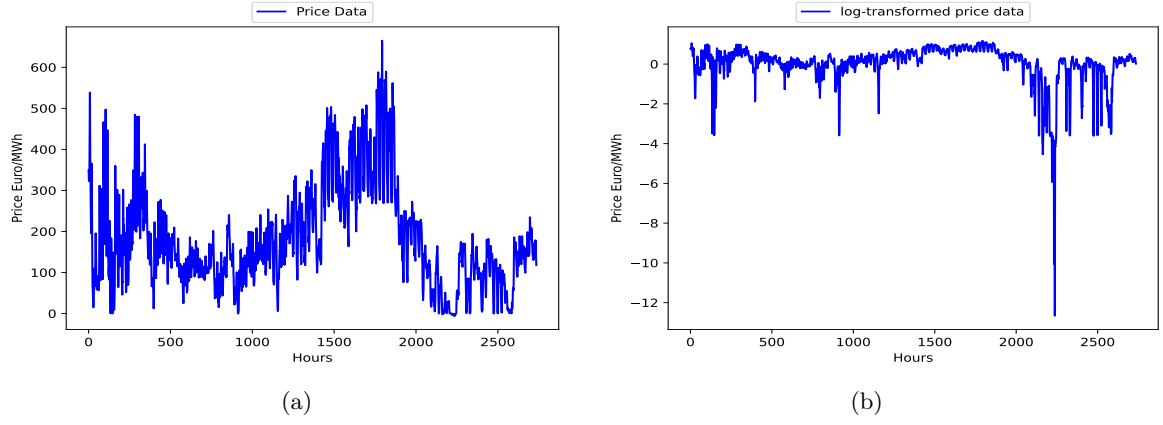


Figure 1: Price Data from 30-Sep-2022 to 21-Jan-2023 (a) real data and (b) log transformed data

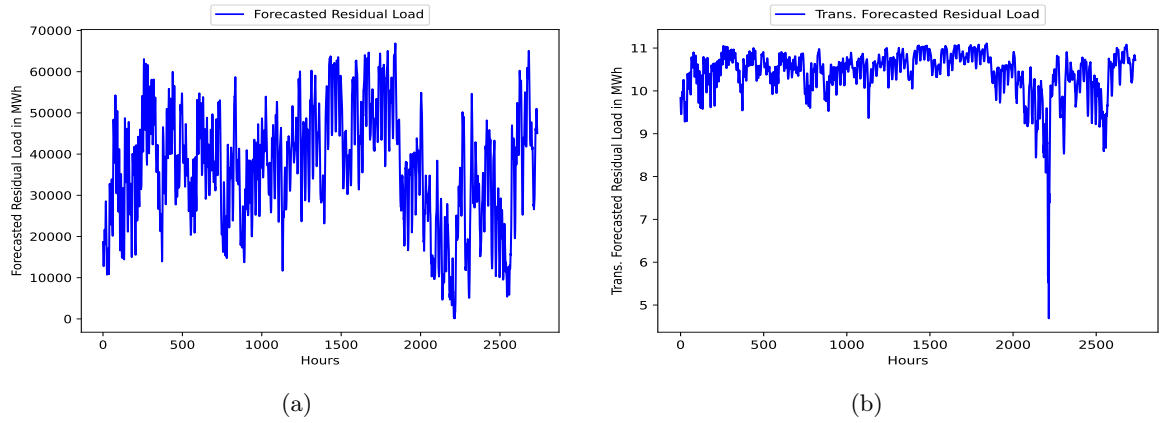


Figure 2: Forecasted Residual Load Data from 30-Sep-2022 to 21-Jan-2023 (a) real data and (b) log transformed data

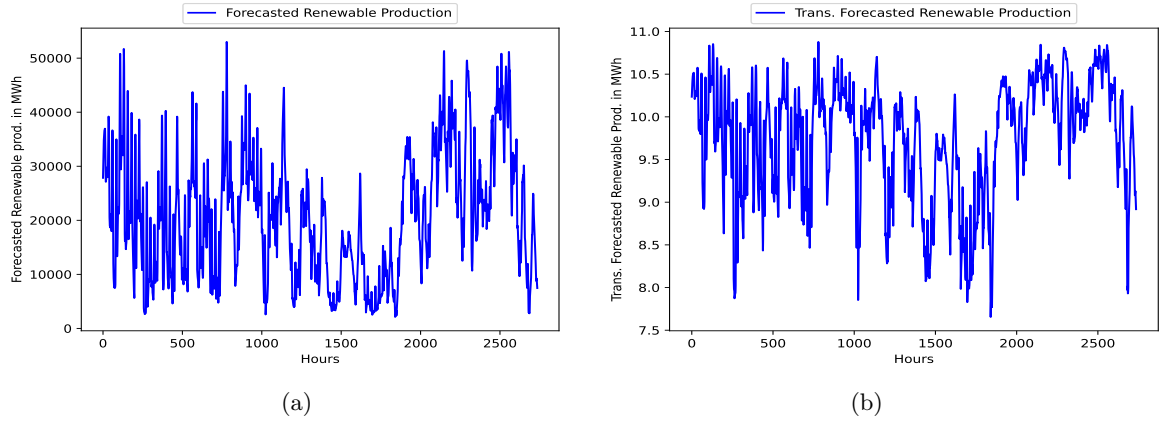


Figure 3: Forecasted Renewable Energy Production Data from 30-Sep-2022 to 21-Jan-2023 (a) real data and (b) log transformed data

as follows:

$$\text{Price Data} = \begin{bmatrix} P_1^{(1)} & P_2^{(1)}, \dots, & P_{24}^{(1)} \\ P_1^{(2)} & P_2^{(2)}, \dots, & P_{24}^{(2)} \\ \vdots & \vdots & \vdots \\ P_1^{(n)} & P_2^{(n)}, \dots, & P_{24}^{(n)} \end{bmatrix}_{n \times 24}$$

↓

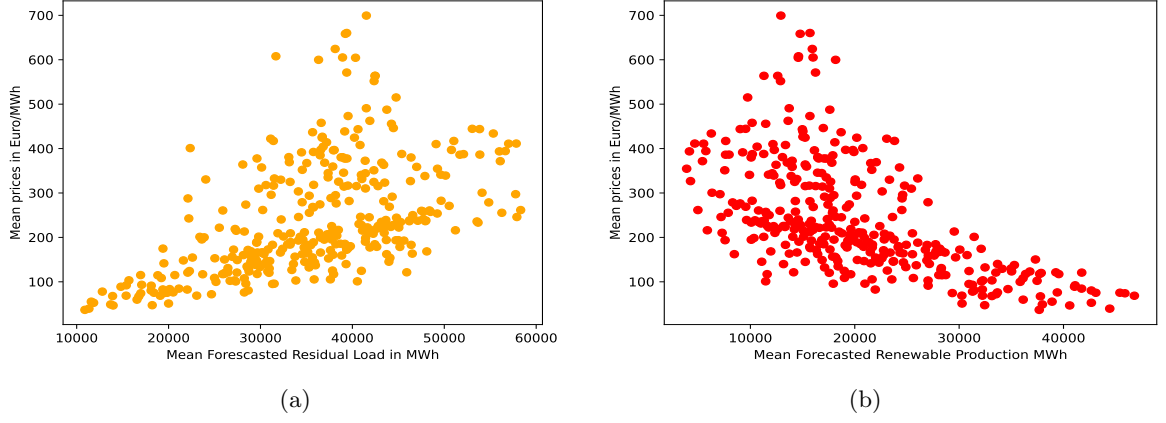


Figure 4: Scatter plot for historic data of (a) daily average of forecasted residual load vs daily average of price and (b) daily average of forecasted total renewable production vs daily average of price, for one year

$$\text{Price data} = \left[P_1^{(1)}, P_2^{(1)}, \dots, P_{24}^{(1)}, P_1^{(2)}, P_2^{(2)}, \dots, P_{24}^{(2)}, \dots, \right. \\ \left. \dots, P_1^{(n)}, P_2^{(n)}, \dots, P_{24}^{(n)} \right]_{1 \times (24 \cdot n)}$$

↓

$$\text{Price data} = [P_1 \ P_2, \dots, \ P_{24 \cdot n}]_{1 \times (24 \cdot n)}$$

Similarly for forecasted load and total renewable production (TRP) data is also arranged as follows:

$$\text{Load data} = [L_1 \ L_2, \dots, \ L_{24 \cdot n}]_{1 \times (24 \cdot n)} \text{ and}$$

$$\text{TRP data} = [R_1 \ R_2, \dots, \ R_{24 \cdot n}]_{1 \times (24 \cdot n)}.$$

4 Gaussian Process Regression

4.1 Gaussian Processes

A stochastic process given by $G = \{P_{\mathbf{t}} : \mathbf{t} \in T\}$, where T is the index set, is said to be a Gaussian process (GP) if and only if for every finite set of indices $\{\mathbf{t}_1, \dots, \mathbf{t}_n\}$ in T the random vector, say, $\mathbf{P} = \{P_{\mathbf{t}_1}, \dots, P_{\mathbf{t}_n}\}$ is jointly Gaussian, i.e. the joint density is given by:

$$f_{\mathbf{P}} = \frac{\exp\left(-\frac{1}{2}(\mathbf{p} - \boldsymbol{\mu}_{\mathbf{P}})^T \boldsymbol{\Sigma}_{\mathbf{P}}^{-1}(\mathbf{p} - \boldsymbol{\mu}_{\mathbf{P}})\right)}{\sqrt{(2\pi)^k |\boldsymbol{\Sigma}_{\mathbf{P}}|}}, \quad (1)$$

where $\boldsymbol{\mu}_{\mathbf{P}}$ is the mean vector of \mathbf{P} given by the mean function $\mathbf{m}(x)$ and $\boldsymbol{\Sigma}_{\mathbf{P}}$ is the covariance matrix given by the covariance function $\bar{K}(\mathbf{t}_i, \mathbf{t}_j)$. These parameters fully explain the Gaussian process [25, 26]. In this work, $T \subset \mathbf{R}^3$ such that $T = \{\mathbf{t}_i : \mathbf{t}_i = [i, L_i, R_i], i = 1, \dots, n\}$ where L_i and R_i are deterministic.

The covariance function $K : T \times T \rightarrow \mathbb{R}$ must be positive semi-definite and symmetric. If $\boldsymbol{\Sigma}_{\mathbf{P}}$ is the covariance matrix formed by K then it follows:

$$\mathbf{x}^T \boldsymbol{\Sigma}_{\mathbf{P}} \mathbf{x} \geq 0 \text{ for any } \mathbf{x} \in \mathbb{R}^n \text{ and } a_{i,j} = a_{j,i} \forall a_{i,j} \in \boldsymbol{\Sigma}_{\mathbf{P}}.$$

The mean function is simply defined as $\mathbf{m}(x) : T \rightarrow \mathbb{R}$.

Covariance functions are often referred to as kernels. In general, a kernel is a bivariate function that is used to transform a function g via a convolution operation C :

$$(Cg)(\mathbf{u}) = \int_T g(\mathbf{v})K(\mathbf{u}, \mathbf{v})d\mathbf{v},$$

where $K(\mathbf{u}, \mathbf{v})$ is the kernel that defines how the function is transformed [27]. Analogously, the covariance function in Gaussian process specifies the process. Hereafter, the terms covariance functions and kernel are used interchangeably.

4.2 Gaussian Process Regression

Classified as a non-parametric Bayesian method [28], GPR is a simple yet powerful method when it comes to model complex relationships in a data set [29]. GPR can be viewed both in terms of standard regression, where the output is the linear combination of the input variables, and as a functional form where the Gaussian process denotes the distribution over functions. The latter is often referred to as the functional space view [22]. In functional space view, the prior distribution is defined by the mean and covariance function, $\mathbf{P} \sim \mathcal{GP}(\boldsymbol{\mu}_P, \boldsymbol{\Sigma}_P)$. Later, using the Bayesian method, the posterior distribution is obtained using the prior and observed data. Since a Gaussian process is fully specified by its mean and covariance functions, given a data set, we only need to estimate the mean vector and the covariance matrix. In practical situations, it is common to assume the mean function as a constant function or zero (this can be achieved by normalization), and then the Gaussian process can be fully specified by the covariance function, which reduces the complexity. The choice of covariance function thereby depends upon the nature of the data, and its parameters (also known as the hyperparameters of the Gaussian process) are then estimated based on the data set. In terms of machine learning, this whole process is called training, which includes estimating the hyperparameter and deriving the covariance matrix using the chosen function. By this step, we have defined the prior and obtained its parameters.

Predicting the value of the random variable (function) at unobserved points, say \mathbf{t}^* , is done by computing the posterior distribution. Let us assume that we have a finite collection $\mathbf{P} = \{P_{\mathbf{t}_1}, \dots, P_{\mathbf{t}_n}\}$ from a Gaussian process, observed at points $T = \{\mathbf{t}_1, \dots, \mathbf{t}_n\}$ with a given covariance function K_{GPR} and mean function $\boldsymbol{\mu}_P$. Given previous observations, we intend to predict at u unobserved points, say $T^* = \{\mathbf{t}_1^*, \dots, \mathbf{t}_u^*\}$, which is denoted by $\mathbf{P}^* = \{P_{\mathbf{t}_1^*}, \dots, P_{\mathbf{t}_u^*}\}$. Assuming that \mathbf{P} and \mathbf{P}^* are jointly Gaussian, their joint distribution reads as follows:

$$\begin{bmatrix} \mathbf{P} \\ \mathbf{P}^* \end{bmatrix} \sim \mathcal{N} \left(\begin{bmatrix} \boldsymbol{\mu}_P \\ \boldsymbol{\mu}_{P^*} \end{bmatrix}, \begin{bmatrix} \boldsymbol{\Sigma}_P + \sigma_n \mathbf{I} & \boldsymbol{\Sigma}_{P, P^*} \\ \boldsymbol{\Sigma}_{P^*, P} & \boldsymbol{\Sigma}_{P^*} \end{bmatrix}_{(n+u) \times (n+u)} \right) \quad (2)$$

where,

- $\boldsymbol{\mu}_P$ and $\boldsymbol{\mu}_{P^*}$ are the respective mean vectors for \mathbf{P} and \mathbf{P}^*
- $\boldsymbol{\Sigma}_P = \{K_{\text{GPR}}(\mathbf{x}_i, \mathbf{x}_j)\}_{i,j=1}^n$ is a covariance matrix from \mathbf{P} and \mathbf{P} of order $n \times n$,
- $\boldsymbol{\Sigma}_{P, P^*} = \{K_{\text{GPR}}(\mathbf{x}_i, \mathbf{x}_j^*)\}_{i=1, \dots, n, j=1, \dots, m}$ is covariance matrix from \mathbf{P} and \mathbf{P}^* of order $n \times u$,
- $\boldsymbol{\Sigma}_{P^*, P} = (\boldsymbol{\Sigma}_{P, P^*})^\top$
- $\boldsymbol{\Sigma}_{P^*} = \{K_{\text{GPR}}(\mathbf{t}_i^*, \mathbf{t}_j^*)\}_{i,j=1}^m$ is covariance matrix from \mathbf{P}^* and \mathbf{P}^* of order $u \times u$,
- \mathbf{I} is the identity matrix of size $n \times n$ and σ_n is the noise variance.

As shown in [30, 31, 22], the respective posterior mean and posterior covariance is given by:

$$\boldsymbol{\mu}^* = \boldsymbol{\mu}_{P^*} + \boldsymbol{\Sigma}_{P^*, P} (\boldsymbol{\Sigma}_P + \sigma_n \mathbf{I})^{-1} (\mathbf{P} - \boldsymbol{\mu}_P), \quad (3)$$

$$\boldsymbol{\Sigma}^* = \boldsymbol{\Sigma}_{P^*} - \boldsymbol{\Sigma}_{P^*, P} (\boldsymbol{\Sigma}_P + \sigma_n \mathbf{I})^{-1} \boldsymbol{\Sigma}_{P, P^*}. \quad (4)$$

Here $\boldsymbol{\mu}^*$ and $\boldsymbol{\Sigma}^*$ are of order $u \times 1$ and $u \times u$, respectively. As discussed earlier, if we assume $\boldsymbol{\mu}_P = \boldsymbol{\mu}_{P^*} = 0$, equation (3) further simplifies to $\boldsymbol{\mu}^* = \boldsymbol{\Sigma}_{P^*, P} (\boldsymbol{\Sigma}_P + \sigma_n \mathbf{I})^{-1} \mathbf{P}$. In [22, Chapter 2] it has been shown that $\boldsymbol{\mu}^*$ is the best estimate of the prediction at the new point \mathbf{t}^* . Similarly, $\boldsymbol{\Sigma}^*$ gives the variance of the prediction, which quantifies the uncertainty associated with the prediction. Therefore the predicted value at the test point $\mathbf{t}_s^* \in T^*$ is μ_s^* , s^{th} component of $\boldsymbol{\mu}^*$, and the uncertainty associated

to the prediction is $\sqrt{\Sigma_{ss}}$. The detailed derivation for the posterior mean and variance can be found in [32, Chapter 2]. The prediction interval at the test point $\mathbf{t}_s^* \in T^*$ is given by:

$$I_{GPR} = [lb_{GPR}, ub_{GPR}], \quad \text{such that} \quad (5)$$

$$lb_{GPR} = \mu_s^* - z_{\alpha/2} \sqrt{\Sigma_{ss}} \quad \text{and} \quad ub_{GPR} = \mu_s^* + z_{\alpha/2} \sqrt{\Sigma_{ss}}.$$

Here $z_{\alpha/2}$ denotes the z-score at a confidence level of $1 - \alpha$, whereby we've exemplarily opted for a 95% confidence interval.

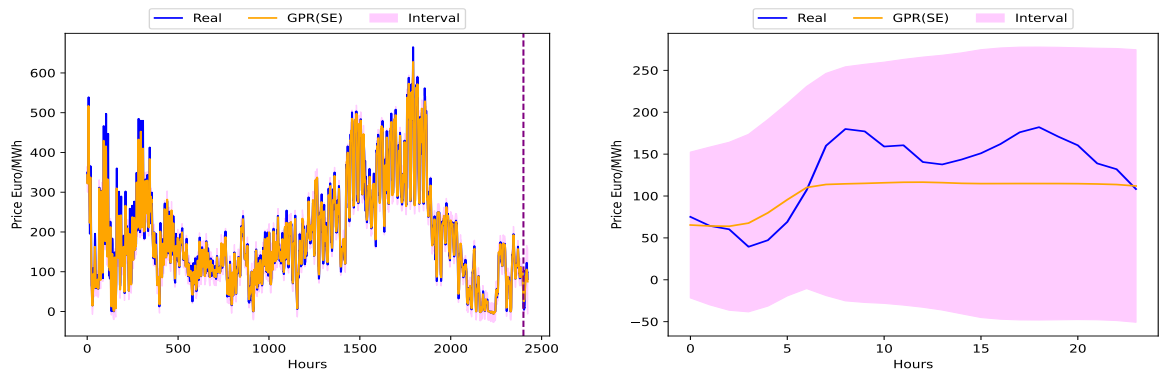
4.2.1 Covariance Functions

Covariance functions show the similarity of two random functions [33] and are of different types e.g. isotropic stationary, anisotropic stationary, locally stationary, non-stationary, etc. For more details, refer to [34, 22] and references therein. Thereby, the chosen covariance function must reflect the structural properties (roughness or smoothness, short- or long-term fluctuations) of the data. At the same time, the so-called decay rate of the function must not be ignored. It determines the speed at which the prediction reverts to the mean of the Gaussian process as the prediction point moves farther away from the observed points (similar to the mean reversion parameter in an Ornstein-Uhlenbeck process). Considering the structure of electricity prices, we chose a squared exponential function and a rational quadratic function for model construction. In the following, we describe both functions and also include sample predictions for illustration. Thereby we forecast prices on 9 January 2023. For prediction, we trained our model with 100 days of past inputs and output. As described above, the inputs are the time index, the forecasted residual load, and the forecasted total renewable production; the output is the price at that time point.

1. Squared Exponential Covariance: This function is also known as the Gaussian covariance function and is appropriate for data sets with local structures. In our case the price of electricity shows repeating patterns in similar situations such as weekends, public holidays, and hours of the day – in other words: seasonality[35]. In [36] the squared exponential covariance function is used to capture the local structure within the data set. The electricity prices are also locally smooth which is another motivation to use a squared exponential covariance in this case. It is defined as follows:

$$K_{se}(\mathbf{t}_i, \mathbf{t}_j) = \sigma_{se}^2 \exp\left(-\frac{\|\mathbf{t}_i - \mathbf{t}_j\|^2}{2\ell_{se}^2}\right).$$

Here, $\|\mathbf{t}_i - \mathbf{t}_j\|$ is the Euclidean distance between points \mathbf{t}_i and \mathbf{t}_j , σ_{se} and ℓ_{se} are the variance and length parameters for the K_{se} respectively, which is considered as hyperparameters of the Gaussian process. These hyperparameters are estimated using the maximum likelihood estimation (MLE). However, as the distance between the points is increased the function decays faster. Because of this, as can be seen in Figures (5a) and (5b), it works well for interpolation but does not perform equally good for prediction outside the training data.



(a) Training data [30-Sep-2022 to 8-Jan-2023]

(b) Prediction of price for 9-Jan-2023

Figure 5: Gaussian Process Regression Using Squared Exponential Covariance Function

2. Rational Quadratic Covariance: Electricity price data exhibit short-term variations due to changes in renewable energy production, cf. [37] whereas long-term changes are observed due to new policy implications, cf. [38]. In such a situation, the rational quadratic function is an appropriate choice. It is defined as follows:

$$K_{rq}(\mathbf{t}_i, \mathbf{t}_j) = \sigma_{rq}^2 \left(1 + \frac{\|\mathbf{t}_i - \mathbf{t}_j\|^2}{2\alpha\ell_{rq}^2} \right)^{-\alpha_{rq}}$$

where \mathbf{x}_i and \mathbf{x}_j are d -dimensional time points.

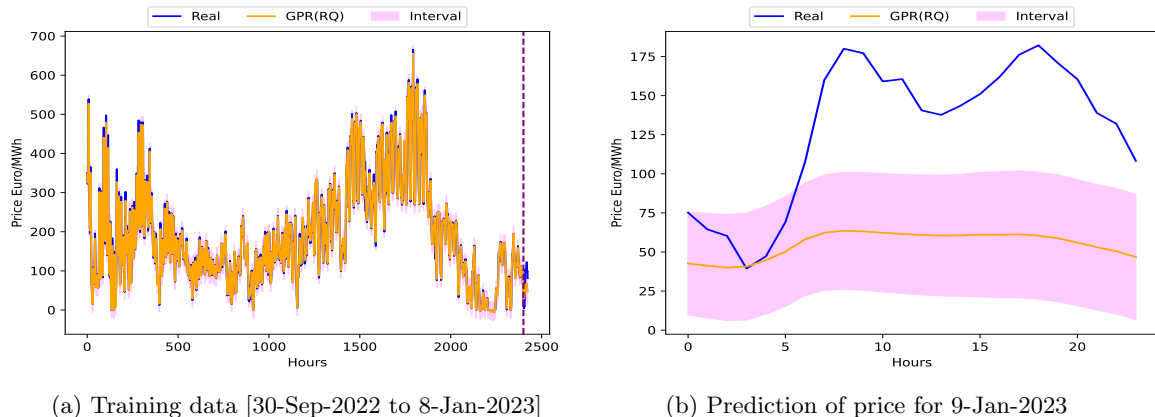


Figure 6: Gaussian Process Regression Using Rational Quadratic Covariance Function

In Figures 6a and 6b, we again see a similar prediction within the training data, but it is even worse than the prediction using the squared exponential model for the new inputs. This is because the training data has many short-range variations which make the model more sensitive and result in misleading prediction.

From Figures 5 and 6, we can see that the predictions using these two covariance functions are aligned with the real values within the training data. However, when the same covariance functions are used to predict the points outside the training data, the results are not similar. In Figure 5b the prediction is better than that shown in Figure 6b. As shown in Figure 6b, the prediction intervals via the rational quadratic covariance function are narrower than those of the squared exponential covariance function in Figure 5b, which is a desirable feature. Nevertheless, the rational quadratic covariance function showed over-flexible towards the short-term variation, due to which the predictions themselves are worse than those of the squared exponential case.

These two covariance functions are not capable of learning information from the training data up to the extent where the prediction is acceptable due to their own limitation which we have explained in Subsection 4.2.2. However, when combining both kernels (as the sum of individual kernels), the situation is different. In Figure 7b we see that with the aggregated kernel generated by adding both individual ones, the prediction is significantly different from the prediction based on individual kernels. In the following section, we have given a mathematical explanation for the observed differences in the performance of these covariance functions.

4.2.2 Analysis of Covariance Functions

In this section, we discuss the local and global behavior of both individual covariance functions mentioned in the previous section, as well as the behavior of their sum. To analyze these, we use partial differentiation with respect to the distance between any two points in the input space denoted by \mathbf{t}_i and \mathbf{t}_j . Since squared exponential and rational quadratic covariance functions are isotropic [34], we can therefore consider $K(\mathbf{t}_i, \mathbf{t}_j) = K(\|\mathbf{t}_i - \mathbf{t}_j\|)$. Assuming $r = \|\mathbf{t}_i - \mathbf{t}_j\|$, we have

$$\begin{aligned} K_{se}(r) &= \sigma_{se}^2 \exp\left(-\frac{r^2}{2\ell_{se}^2}\right) \\ \implies \frac{\partial K_{se}(r)}{\partial r} &= \sigma_{se}^2 \left(-\frac{r}{\ell_{se}^2}\right) \exp\left(-\frac{r^2}{2\ell_{se}^2}\right) \text{ and} \end{aligned} \tag{6}$$

$$\frac{\partial^2 K_{se}(r)}{\partial r^2} = \sigma_{se}^2 \left(\frac{r^2}{\ell_{se}^4} - \frac{1}{\ell_{se}^2} \right) \exp \left(-\frac{r^2}{2\ell_{se}^2} \right). \quad (7)$$

Analogously, for the rational quadratic function we obtain:

$$\frac{\partial K_{rq}(r)}{\partial r} = -\frac{r \cdot \sigma_{rq}^2}{\ell_{rq}^2} \cdot \left(1 + \frac{r^2}{2\alpha_{rq}\ell_{rq}^2} \right)^{-\alpha_{rq}-1} \quad \text{and} \quad (8)$$

$$\begin{aligned} \frac{\partial^2 K_{rq}(r)}{\partial r^2} &= \frac{\sigma_{rq}^2 \cdot r^2 \cdot (\alpha_{rq} + 1)}{(\alpha_{rq}\ell_{rq}^4)} \cdot \left(1 + \frac{r^2}{2\alpha_{rq}\ell_{rq}^2} \right)^{-\alpha_{rq}-2} \\ &\quad - \left(\frac{\sigma_{rq}}{\ell_{rq}} \right)^2 \cdot \left(1 + \frac{r^2}{2\alpha_{rq}\ell_{rq}^2} \right)^{-\alpha_{rq}-1} \end{aligned} \quad (9)$$

Similarly, for $K = K_{se} + K_{rq}$ we have

$$\begin{aligned} \frac{\partial K(r)}{\partial r} &= \frac{\partial K_{se}(r)}{\partial r} + \frac{\partial K_{rq}(r)}{\partial r} \\ &= \sigma_{se}^2 \left(-\frac{r}{\ell_{se}^2} \right) \exp \left(-\frac{r^2}{2\ell_{se}^2} \right) - \frac{r \cdot \sigma_{rq}^2}{\ell_{rq}^2} \cdot \left(1 + \frac{r^2}{2\alpha_{rq}\ell_{rq}^2} \right)^{-\alpha_{rq}-1} \quad \text{and} \end{aligned} \quad (10)$$

$$\begin{aligned} \frac{\partial^2 K(r)}{\partial r^2} &= \sigma_{se}^2 \left(\frac{r^2}{\ell_{se}^4} - \frac{1}{\ell_{se}^2} \right) \exp \left(-\frac{r^2}{2\ell_{se}^2} \right) \\ &\quad + \frac{\sigma_{rq}^2 \cdot r^2 \cdot (\alpha_{rq} + 1)}{(\alpha_{rq}\ell_{rq}^4)} \cdot \left(1 + \frac{r^2}{2\alpha_{rq}\ell_{rq}^2} \right)^{-\alpha_{rq}-2} \\ &\quad - \left(\frac{\sigma_{rq}}{\ell_{rq}} \right)^2 \cdot \left(1 + \frac{r^2}{2\alpha_{rq}\ell_{rq}^2} \right)^{-\alpha_{rq}-1}. \end{aligned} \quad (11)$$

From Equation (6) it is clear that the change in squared exponential covariance function with respect to the distance between two points (we refer to this as sensitivity) is very small when two points in the input space are close to each other. Specifically: $\frac{\partial K_{se}(r)}{\partial r} \rightarrow 0$ as $r \rightarrow 0$. For larger distances, the change in the covariance function becomes less significant because of the exponential factor in the RHS of Equation (6), $\exp(-\frac{r^2}{2\ell_{se}^2})$ tends to 0 as $r \rightarrow \infty$. The length scale in the training data, estimated over the training input and output, also helps us give information about how fast or slow our covariance function decays. From Equation (6) we can see that the bigger the ℓ_{se} , the slower will be the decay. For the rational quadratic covariance function, the case is similar when two input points are closer because: $\frac{\partial K_{rq}(r)}{\partial r} \rightarrow 0$ as $r \rightarrow 0$, however for the far apart points, the decay is slower due to the polynomial term in the denominator:

$$\frac{1}{\left(1 + \frac{r^2}{2\alpha_{rq}\ell_{rq}^2} \right)^{(\alpha_{rq}+1)}} \rightarrow 0 \quad \text{as } r \rightarrow \infty.$$

Additionally, in the rational quadratic case, α gives more flexibility to look after the sensitivity of the rational quadratic function. From Equation (8) we see that the smaller the α , the slower the decay. Similarly, from Equation (7) we see that change in the structure (curvature) is very fast since the exponential term in the RHS dominates as the distance between the points in the input space increases and converges to zero however it is smooth. For rational quadratic covariance function, this convergence is comparatively slower than the squared exponential due to presence of polynomial terms, but the smoothness varies with α_{rq} which can be seen in Equation (9). To verify the theoretical findings from equations (6) to (11), we tested these covariance functions on the GPR inputs. The parameters of the covariance function are estimated using 3-dimensional input data and 1-dimensional output data taken from the past 100 days. For illustration, we took data from 30 September 2022 to 7 January 2023. The input consisted of scaled hour, log-transformed forecasted residual load, and log-transformed forecasted total renewable energy production, whereas the outputs are the price of electricity on a particular hour.

We see from Figure 8a that most of the off-diagonal values in the covariance matrix obtained using the squared exponential function, with $\ell_{se} = 0.7517$, are close to zero, which is justified by equation (6) and equation (7), inferring that the far apart points have near-zero covariance. In Figure 8b, which displays the rational quadratic function with $\ell_{rq} = 0.2067$, we do not see as many zeros as in the

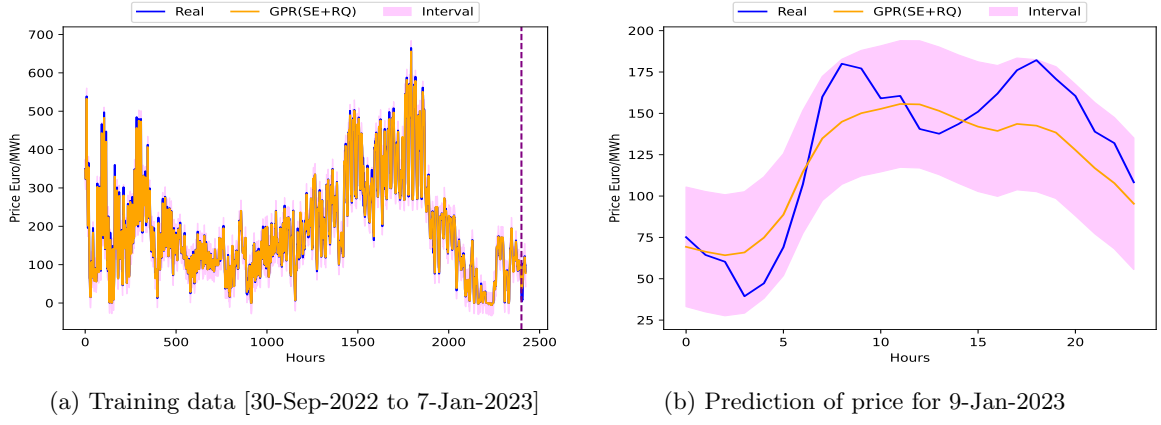


Figure 7: Gaussian process regression using combination of RBF and Rat-Quad Kernel on electricity data

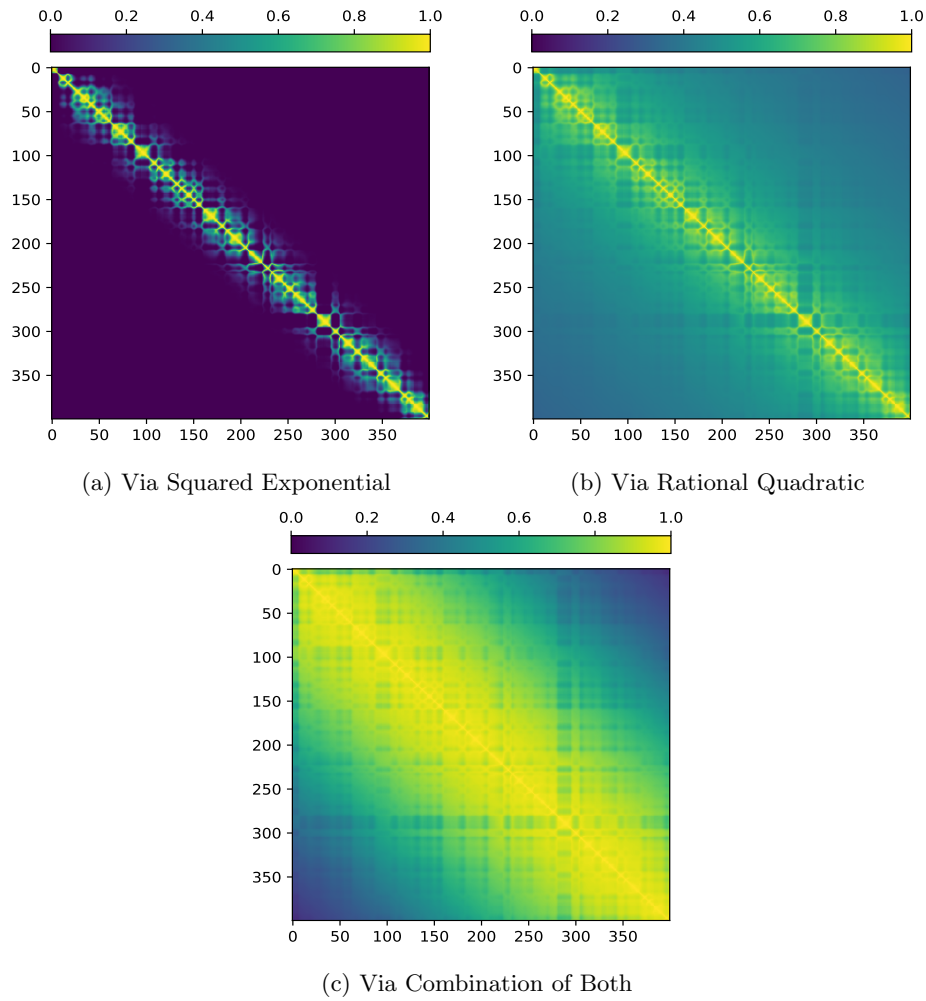


Figure 8: Behaviour of Covariance Functions

squared exponential case since the decay is slower, which we already discussed earlier. Although in terms of rational long-range dependence, the rational quadratic covariance function is performing better than the squared exponential covariance function, it can be solely considered for modeling purposes because of the smoothness property for which a squared exponential kernel is better. Figures 5 and 6 give us a reference for the result of using the individual covariance function solely for the regression. Both covariance functions have drawbacks and advantages, and these limitations can be reduced by

combining these two functions by a summation. In equations (10), (11) and in Figure 7, it is evident that the covariance function $K = K_{se} + K_{rq}$ is capable of capturing the smoothness and long-range dependencies, which is very evident from (8c).

In addition, in Appendix (10) we have discussed the capability of $K = K_{se} + K_{rq}$ to capture the periodic behavior in the data. Also, for uncertainty (posterior variance) associated with the prediction, we can infer from Equation (4) and the analysis of the covariance function that the posterior variance in the case of the combined covariance function includes the variance of both covariance functions. This, in turn, leads to better adjustment of the variance in the input space.

There is a wide range of other covariance functions such as the exponential covariance function, the polynomial covariance function, or functions belonging to the maternal family [39]. However, the combination of squared exponential and rational quadratic maintains a balance for required short-range and long-range changes and dependencies.

The prediction shown in Figure 9a is the comparison of GPR with a combination of squared exponential and rational quadratic covariance functions. For the sake of a clear comparison, we have shown the prediction only for the second week of January 2023. As shown in Figure 9b, when the GPR model is used to predict a larger number of days, particularly, from January to December of the same year, we observed some predictions in which the difference between the real and predicted prices is comparatively higher than the other prediction in the same time period. The model made such a prediction with a higher error because of overfitting due to outliers or noise in the training data. One approach to solving this problem of sudden unrealistic predictions is to remove the outliers and noise in the dataset before training the model. However, several researchers warn that erroneously removing outliers can distort the structure of the dataset and affect model training, cf. [40, 41, 42]. An alternative is to choose a model that is comparatively robust to overfitting. We discuss this approach in the next section.

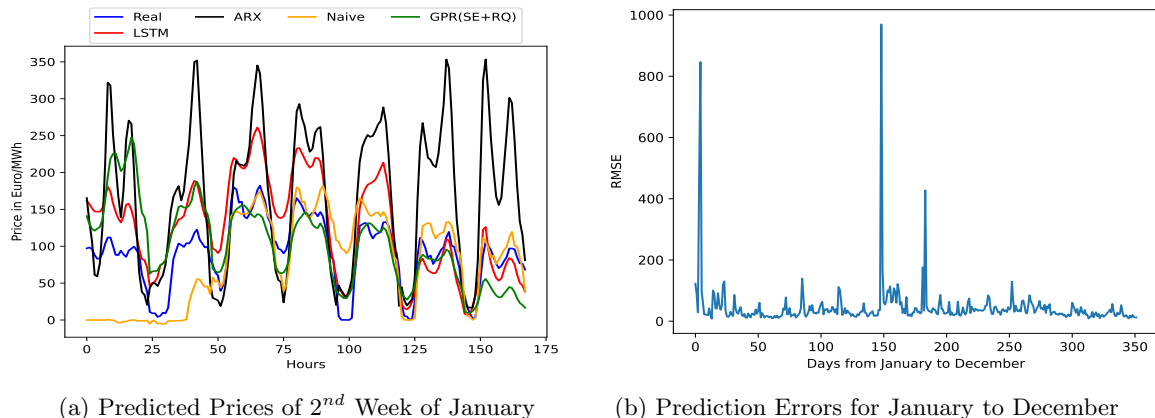


Figure 9: Gaussian Process Regression Comparison

5 Support Vector Regression

To overcome the problem arising due to the overfitting due to the presence of outliers or noise in the training data, we use SVR to predict the price using the same dataset. SVR is effective in handling high-dimensional feature spaces and is robust to overfitting, making it a suitable choice for our data, given its characteristics [43, 44, 45]. After the prediction via both GPR and SVR, we combine both of the predictions by penalizing the prediction with higher error which we have discussed in Section (6) and this improves the overall prediction. GPR predictions are associated with uncertainty, and hence give us information about the prediction interval based on the posterior variance. SVR prediction, in turn, is a statistic and this probabilistic approach for prediction interval cannot be directly obtained. The solution is to apply SVR in the context of conformal prediction.

5.1 Kernel Based Support Vector Regression

Support vector machines belong to the supervised machine learning model based on margin maximization and are primarily used for classification problems [46]. However, there is also substantial literature

on SVM being used for regression problems, and in this case, we call it support vector regression. The method is particularly useful when the relationship of the input variables with the output variables are non-linear. Here we give a brief mathematical introduction, for more information see [23].

Let $T = \{\mathbf{t}_1, \dots, \mathbf{t}_n\}$ being d -dimensional the inputs and $\{P_1, \dots, P_n\}$ are corresponding outputs. In our work we have $d = 3$. We are aiming towards predicting the output at $T^* = \{\mathbf{t}_1^*, \dots, \mathbf{t}_m^*\}$. The basic idea of SVM is to find a function $f(\mathbf{t})$ for input \mathbf{t} which is ϵ -deviated from the actual output. For simplicity, we first present a case where the input and output share a linear relationship, and such a situation the function can be formulated as follows:

$$f(\mathbf{t}) = \langle \mathbf{w}, \mathbf{t} \rangle + b, \mathbf{t} \in T, b \in \mathbb{R}, \quad (12)$$

where \mathbf{w} is a vector normal to the function, which eventually is a plane, and $\langle \cdot, \cdot \rangle$ denotes the dot product. For, $f(\mathbf{t})$ to be a suitable function, the difference of the real output $\{P_i\}_{i=1}^n$ and value of the function $f(\mathbf{t}_i), i = 1, \dots, n$ can be up to ϵ and the \mathbf{w} should be flat which in the linear case means that it should be sufficiently small. This can be formulated as an optimization problem which reads:

$$\begin{aligned} \min \quad & \frac{1}{2} \|\mathbf{w}\|^2 \\ \text{subjected to} \quad & \begin{cases} P_i - \langle \mathbf{w}, \mathbf{t} \rangle \leq \epsilon \\ \langle \mathbf{w}, \mathbf{t} \rangle - P_i \leq \epsilon \end{cases} \end{aligned} \quad (13)$$

Problem (13) is convex and we assume it is feasible. Practically, there may arise the case of infeasibility and to deal with such condition, one can introduce the slack variables ξ and ξ^* as done in [47] and the optimization problem (13) can be reformulated as follows:

$$\begin{aligned} \min_{\mathbf{w}, \mathbf{b}, \xi, \xi^*} \quad & \frac{1}{2} \|\mathbf{w}\|^2 + C \sum_{i=1}^n (\xi_i + \xi_i^*) \\ \text{subjected to} \quad & \begin{cases} P_i - \langle \mathbf{w}, \mathbf{t} \rangle \leq \epsilon + \xi_i \\ \langle \mathbf{w}, \mathbf{t} \rangle - P_i \leq \epsilon + \xi_i^* \\ \xi_i, \xi_i^* \geq 0 \end{cases} \end{aligned} \quad (14)$$

Using the Lagrangian method and constructing the dual of the problem (14), it can be solved as done in [48]. In the case of input and output having a non-linear relationship, the function can be defined as follows:

$$f(\mathbf{t}) = \sum_{i=1}^n (\alpha_i - \alpha_i^*) K_{SVR}(\mathbf{t}_i, \mathbf{t}) + b, \quad (15)$$

where, α_i and α_i^* are the Lagrange multipliers for Problem (14) and $K_{SVR}(\mathbf{t}_i, \mathbf{t})$ is a kernel. The formulation of the function in Equation 15 is often referred to as *kernel trick*. Moreover, while formulating the Lagrangian form of Eq. (14), two more Lagrange multipliers appear but they can be eliminated [23, section 1.3]. The kernel trick method is useful because in this method the the kernel K_{SVR} maps the d -dimensional input to a higher dimensional space and then the mapped input is approximately linear to the output, which reduces the complexity. The mapping of input to higher dimensional data is implicit as follows:

$$K_{SVR}(m, n) = \langle \phi(m), \phi(n) \rangle \quad (16)$$

where $\phi : T \rightarrow \mathbb{R}^l$, and $l \gg d$. It is important to notice that the kernel must be in the form of a dot product of functions that are mapping the input to higher dimensional space as shown in Equation (16) [23, Section 2.3, Theorem 2]. Since the kernel only depends on the dot product of the inputs, the explicit form of ϕ is not required.

In Figure 10, we have illustrated the prediction of electricity prices using SVR with squared exponential kernel. We have also tested the performance of different kernels for larger number of dates which we have shown in Appendix (9). The inputs and outputs for training the SVR model are the same as we used for the GPR. We see that the SVR is not performing very well even with the training dataset. This is because, while training over the data points, we allow a certain deviation ϵ from the real data. One can argue that for a better fit with the data we can choose $\epsilon = 0$. However, this is rarely done because in that case, the SVR model will be more prone to including noise in the data as a data structure which leads to over-fitting in that case.

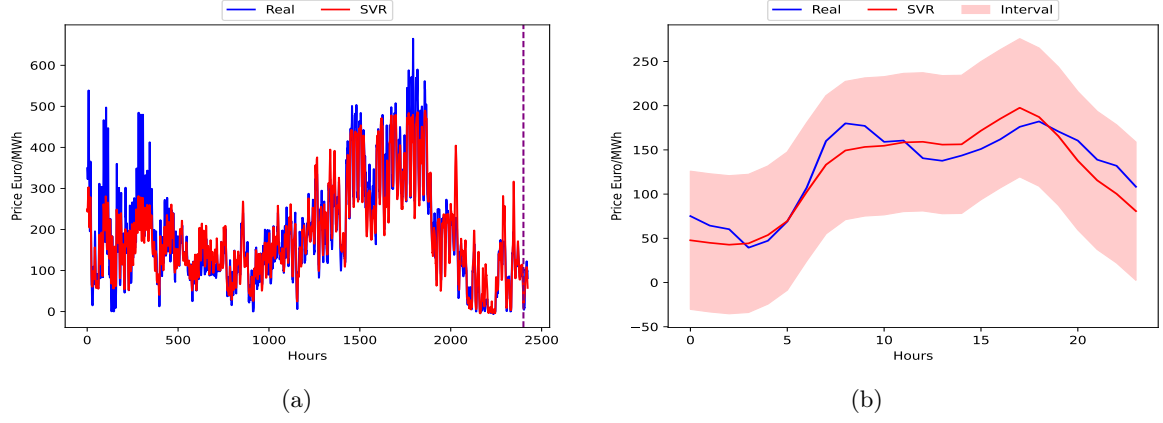


Figure 10: Support vector Regression Using Squared Exponential Kernel on Electricity data:
(a) Training Till the Red-Line and (b) Predicting for One Day (9-Jan-2023)

5.2 Prediction Interval for Support Vector Regression

For computing conformal predictions we follow [49]. Let $\{P_1, \dots, P_n\}$ be the true values and its corresponding predicted values via SVR is $\{\hat{P}_1, \dots, \hat{P}_n\}$ for the inputs $T = \{\mathbf{t}_1, \dots, \mathbf{t}_n\}$. Analogously to GPR, the output at a new point $\mathbf{t}^* \in T^*$ is denoted by P^* . In order to construct the prediction interval for output at a new time instance, \mathbf{t}^* , the non-conformity values. In simple terms non-conformity values tell us how different a test point is compared to a set of training points [49]. It is denoted by α , and is calculated as follows:

$$\alpha_i = |P_i - \hat{P}_i| \text{ and} \quad (17)$$

$$\alpha_j^* = |P^* - \tilde{P}_j| \text{ where } \tilde{P}_j \in [P_{low}, P_{up}], \quad (18)$$

Since we do not have access to the real value for P^* , on the basis of the training output, we assume that \tilde{P}_j belongs to the interval $[P_{low} = \mu_{svr} - \nu\sigma_{svr}, P_{up} = \mu_{svr} + \nu\sigma_{svr}]$, where μ_{svr} and σ_{svr} are the mean and standard deviation of the training outputs. We have chosen $j = 1, \dots, 500$ for \tilde{P}_j which are uniformly distributed between P_{low} and P_{up} . For the 95% confidence interval we compute the proportionality values, denoted as Γ_j , as follows:

$$\Gamma_j = \frac{n\{\alpha_i : \alpha_i \geq \alpha_j^*, i = 1, \dots, n\}}{n+1}, \quad \forall j = 1, \dots, 500, \quad (19)$$

where $n\{\cdot\}$ denotes a set's cardinality and n is the number of training outputs. This proportionality value gives the fraction of test points that are equally or more distinct from the training data. Next, we construct a set Π as follows:

$$\Pi = \left\{ \tilde{P}_j : \frac{n\{\alpha_i : \alpha_i \geq |P^* - \tilde{P}_j|, i = 1, \dots, n\}}{n+1} \geq 0.05, \forall j = 1, \dots, 500 \right\}.$$

The prediction interval for P^* is given by:

$$\begin{aligned} I_{SVR} &= [lb_{SVR}, ub_{SVR}] \quad \text{such that} \\ lb_{SVR} &= \min(\Pi) \text{ and } ub_{SVR} = \max(\Pi) \end{aligned}$$

Note that we assume that the data here is exchangeable, which is a weaker assumption than being independently identically distributed.

Since \tilde{P}_j s are drawn uniformly, the interval I_{SVR} is dependent upon \tilde{P}_j s, so for the robustness of the interval, we use bootstrapping and repeatedly generate \tilde{P}_j s. For each repetition, we have one $I_{SVR}^k = [lb_{SVR}^{(k)}, ub_{SVR}^{(k)}], k = 1, \dots, s$ and then compute the average of the lower and upper bounds of each I_{SVR} as a final prediction interval which reads as follows:

$$\begin{aligned} I_{SVR}^{BS} &= [lb_{SVR}^{BS}, ub_{SVR}^{BS}] \text{ such that,} \quad (20) \\ lb_{SVR}^{BS} &= \frac{1}{s} \sum_{k=1}^s lb_{SVR}^{(k)} \text{ and } ub_{SVR}^{BS} = \frac{1}{s} \sum_{k=1}^s ub_{SVR}^{(k)} \end{aligned}$$

6 A Hybrid Model for Electricity Price Prediction

6.1 The Hybrid Model

In this section, we propose a hybrid model that linearly combines GPR-based and SVR-based prediction. SVR, being better in dealing with outliers [50, 51, 52, 53] helps assign lesser weights to GPR prediction in times of predictions being affected by outliers in the training data. As mentioned in Section 4, we choose a three-dimensional input and we have training data as follows:

$$\mathbf{P}_{\text{train}} = \{P_{\mathbf{t}_i}, : \mathbf{t}_i = [i, L_i, R_i] \in T \subset \mathbb{R}^3, \forall i = 1, \dots, n\}. \quad (21)$$

Here n is the number of observable values, i.e. number of training data. We have transformed each hour to a value between 0 and 100 to avoid numerical inconsistencies in the case of large n . We define a hybrid model for the price prediction as a linear combination of the individual predictions, which reads as follows:

$$\mathbf{P}_{\mathbf{x}^*} = \lambda_1 \underbrace{\left(\Sigma_{\mathbf{P}^*, \mathbf{P}} (\Sigma_{\mathbf{P}} + \sigma_n \mathbf{I})^{-1} \mathbf{P} \right)}_{\text{Gaussian process regression}} + \lambda_2 \overbrace{\left(\sum_{i=1}^n (\alpha_i - \alpha_i^*) K_{SVR}(\mathbf{x}_i, \mathbf{x}) + b \right)}^{\text{Support vector regression}}, \quad (22)$$

where the first expression on the right-hand side denotes the GPR prediction and the second the SVR prediction. The parameters of the hybrid model are estimated individually. The weights λ_1 and λ_2 are calculated by evaluating the error using the validation set (see Subsection 6.2). The prediction interval of the individual models are combined using the weights λ_1 and λ_2 as follows:

$$I_{GPR+SVR} = [lb_{com}, ub_{com}] \text{ such that,} \quad (23)$$

$$lb_{com} = \lambda_1 lb_{GPR} + \lambda_2 lb_{SVR}^{BS} \text{ and } ub_{com} = \lambda_1 ub_{GPR} + \lambda_2 ub_{SVR}^{BS}$$

For the GPR part in Equation (22), the covariance matrix $\Sigma_{\mathbf{P}}$ is given by K_{GPR} , which is the sum of squared exponential covariance function and rational quadratic function as follows:

$$\begin{aligned} K_{GPR}(\mathbf{t}_i, \mathbf{t}_j) &= K_{se}(\mathbf{t}_i, \mathbf{t}_j) + K_{rq}(\mathbf{t}_i, \mathbf{t}_j) \\ &= \sigma_{se}^2 \exp\left(-\frac{\|\mathbf{t}_i - \mathbf{t}_j\|^2}{2\ell_{se}^2}\right) + \sigma_{rq}^2 \left(1 + \frac{\|\mathbf{t}_i - \mathbf{t}_j\|^2}{2\alpha\ell_{rq}}\right)^{-\alpha}, \end{aligned} \quad (24)$$

where ℓ_{se} and ℓ_{rq} are the length scale for squared exponential and rational quadratic kernel respectively and σ_{se} and σ_{rq} are the variance parameters for squared exponential and rational quadratic kernel, respectively. These are the hyperparameters of Gaussian process models which are estimated using $\mathbf{P}_{\text{train}}$, via MLE. The marginal likelihood function $\mathbf{P}_{\text{train}}$ reads as follows:

$$p(\mathbf{P}_{\text{train}}|T, \theta) = \mathcal{N}(\mathbf{P}_{\text{train}}|\mathbf{0}, K_{GPR} + \sigma_n^2 \mathbf{I}). \quad (25)$$

Here, $\theta = (\sigma_{se}^2, \ell_{se}, \sigma_{rq}^2, \ell_{rq}, \alpha, \sigma_n^2)$, \mathbf{I} is the identity matrix and σ_n^2 is the variance for the noise term. It is important to include the noise term in the prior because we assume that the data is noisy. The log marginal likelihood (LML) is given by:

$$\begin{aligned} \log [p(\mathbf{P}_{\text{train}}|T, \theta)] &= -\frac{1}{2} \mathbf{P}_{\text{train}}^\top (K_{GPR} + \sigma_n^2 \mathbf{I})^{-1} \mathbf{P}_{\text{train}} \\ &\quad - \frac{1}{2} \log |K_{GPR} + \sigma_n^2 \mathbf{I}| - \frac{n}{2} \log 2\pi. \end{aligned} \quad (26)$$

By differentiating the log marginal likelihood with respect to the parameters individually and setting them to zero we obtain parameter estimates.

For the SVR we use the same input to train the model, however, the kernel is changed. Both GPR and SVR are kernel-based approaches but the way both method uses the kernel is different. In GPR, the kernel defines the smoothness and variability of the predicting distribution whereas in SVR the kernel is used to transform the input space to a higher dimensional space in which the input and output may share an approximately linear relationship. Based on the performance we choose the best kernel among a set of kernels, which consists of the squared exponential, the polynomial, the sigmoid, and the linear kernel. We use grid search to choose the kernel parameters for every prediction. For computing b in the final model given in (22) we apply the Karush Kuhn Tucker (KKT) condition [54]. For a detailed derivation of b , please refer to [55].

6.2 Weights Computation

The values of λ_1 and λ_2 in Equation (22) are computed based performance of each individual model on the validation data. For this let the validation data for any day d be denoted by P^d . Let the GPR prediction be P^{GPR} and the SVR prediction be P^{SVR} . We use the root mean square error to evaluate the performance of each predictions by individual model and denote them as $RMSE_{GPR}$ and $RMSE_{SVR}$. In order to assign higher weights to the model that shows lower RMSE values the errors are converted to weights as follows:

$$W_{GPR} = \frac{1}{RMSE_{GPR}} \text{ and } W_{SVR} = \frac{1}{RMSE_{SVR}},$$

which after normalizing yields λ_1 and λ_2 as follows:

$$\lambda_1 = \frac{W_{GPR}}{W_{GPR} + W_{SVR}} \text{ and } \lambda_2 = \frac{W_{SVR}}{W_{GPR} + W_{SVR}}.$$

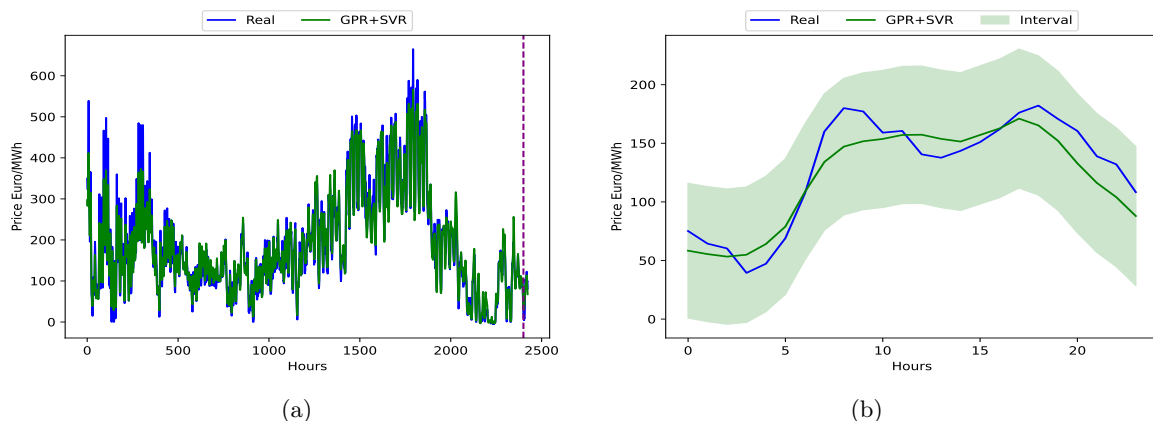


Figure 11: Hybrid model predicting on (a) training till the red-line and (b) test data for one day

7 Numerical Results

We test our new hybrid model on German power prices for the years 2021-2023. However, the main focus lies on 2023 as structural breaks reduce the explanatory power of older data. The seasonal comparison (summer, winter, autumn, and spring) is only conducted for 2023 and the predictions for 2021 and 2022 serve primarily to test the model's reliability. The GPR and SVR models are trained using the past 100 days of data, which consists of 2400 data points. The training data is constructed as outlined in Equation (21), where the input for each prediction is represented as, $\mathbf{t}_i = [i, L_i, R_i]$. Here L_i and R_i are the second and third components, which are centered and log-transformed. We denote the training input and training output as train_{in} and train_{out} respectively:

$$\text{train}_{in} = (\mathbf{t}_1, \dots, \mathbf{t}_{2400}) \text{ and } \text{train}_{out} = (P_1, \dots, P_{2400}).$$

The hyperparameters of the Gaussian process are estimated using MLE, as shown in equation (26) based on train_{in} and train_{out} . Since the training data is centered and log-transformed, the model parameters are learned on this transformed scale, and predictions are subsequently re-transformed back to the original scale. For SVR the same training data is used to choose the parameters for the squared exponential kernel using grid search. For the search process, we choose $\epsilon \in [0.001, 0.1, 0.1]$, $C \in [0.1, 1, 10]$, $\hat{c} \in [0, 1, 10]$. The comparison for prediction via SVR using different kernels is shown in Section (9).

Both trained GPR and the SVR models are used to predict the next 48 data points using the same prediction inputs which we denote here as pred_{in} . From the predicted output, denoted as pred_{out} , the first 24 predicted output data are used for validation and weight evaluation for the GPR and SVR models which later is used in the final prediction. For example, if we are predicting the price of

2-Jan-2023, we take the hourly data from 23-Sep-2022 to 31-Dec-2022 as a vector of 2400 data points and predict the price of 1-Jan-2023 and 2-Jan-2023 where 1-Jan-2023 is used for validation.

$$\text{pred}_{in} = (\mathbf{t}_{2401}, \dots, \mathbf{t}_{2448}) \text{ and } \text{pred}_{out} = (P_{2401}, \dots, P_{2448})$$

Since we are using the Gaussian process as a regression model in one of the predicting models, taking the data points that are significantly distant from the last training points is not feasible since the Gaussian process is mean reverting. If we choose a bigger validation set, for example, 48 or 72 data points (2 or 3 days) as validation data, then the error of the GPR will be higher and less weight will be given to GPR model and maximum weight will be assigned to the SVR model. Hence SVR will dominate the prediction, which is not desired.

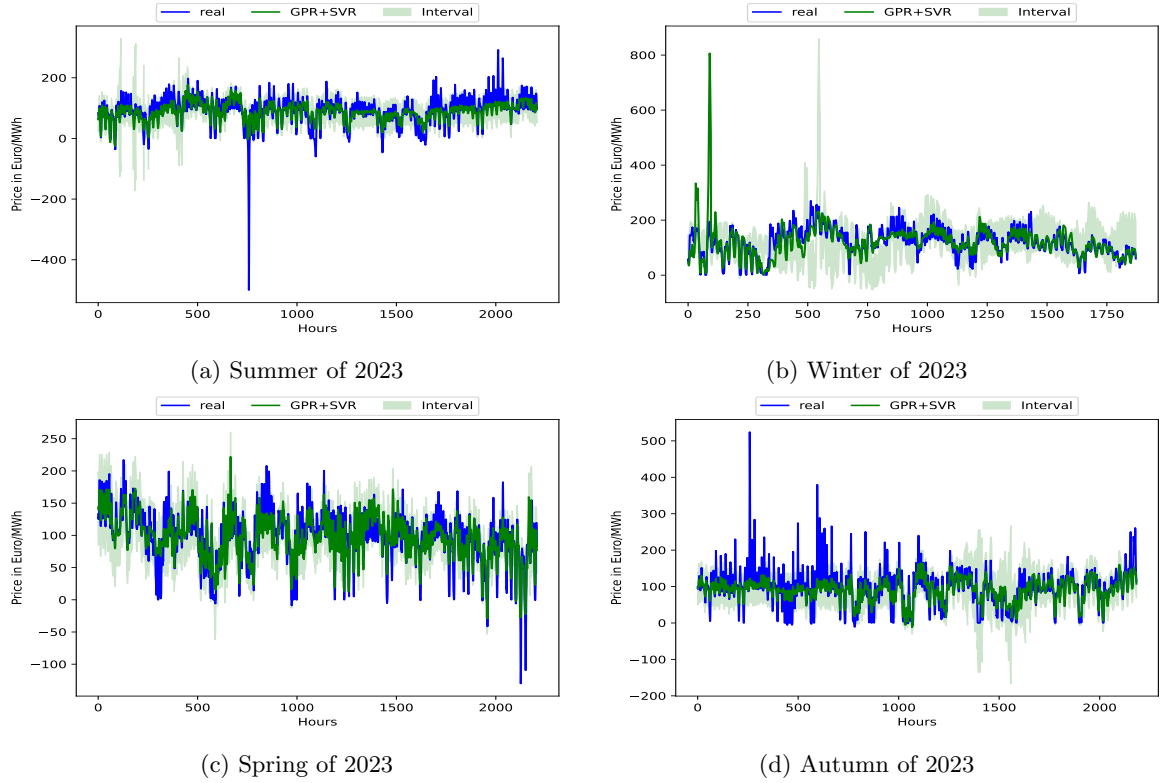


Figure 12: Season-wise comparison

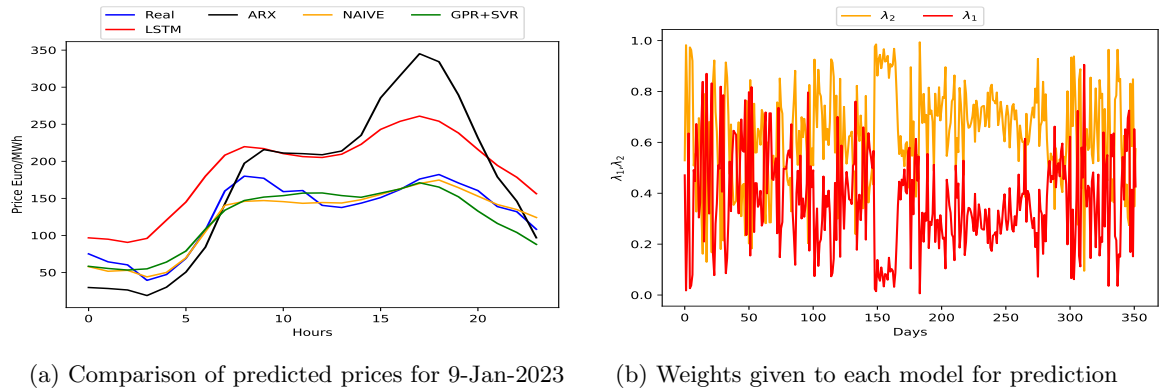


Figure 13: Hybrid model Performance

For a visual comparison, we have only shown the prediction of 14 days prices (consecutive days chosen at random) in Figure (14), which shows the comparison of the real price with the predictions via hybrid model and the benchmark models: Autoregressive Exogenous model (ARX), the naive model

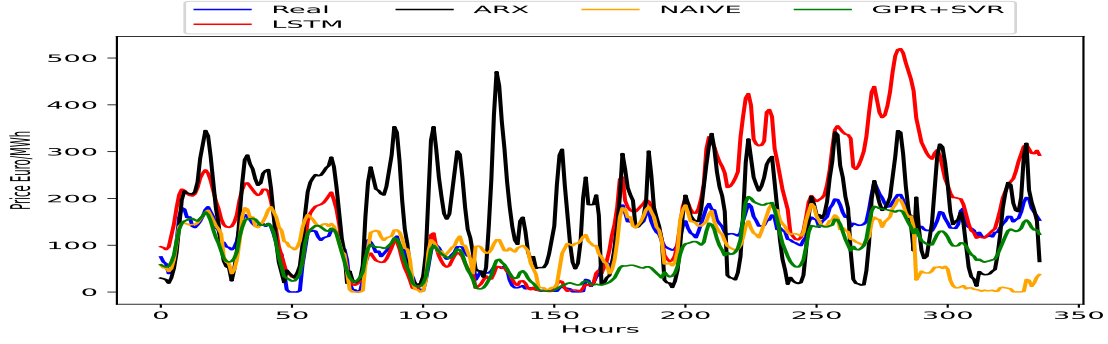


Figure 14: Illustration of 9-Jan-2023 to 22-Jan-2023

and long short-term memory (LSTM) model. This figure shows that the hybrid model is performing better than the benchmark models we have used. However, for the year 2023 the model performance is evaluated using 352 days that is from 01-Jan-2023 to 19-Dec-2023. In Figure (12) we show the prediction based on the hybrid model for four seasons in Germany, namely summer (June to August), winter (January, February, and December of the same year), autumn (September to November) and spring (March to May). From Figures (12a, 12b, 12c, 12d), we see that on average the predictions are aligned with the real data. For a few days in each season, the prediction for some time points is comparatively worse than the predictions of prices in its neighboring time points, however, such cases are not repetitive. This particularly happens when the training data has suddenly very high or very low prices for very short intervals. In such cases the model could not capture the pattern within that short interval and the prediction is relatively poor.

7.1 Error Analysis

Our hybrid model’s performance is evaluated by comparing its prediction to results from the LSTM, the NAIVE, and the ARX model. As previously stated, the primary focus of this study is on the year 2023. However, error analysis was also conducted for the years 2021 and 2022. The RMSE and the mean absolute error (MAE) are used to evaluate the model performance and are defined here as follows:

$$\text{RMSE}_i = \sqrt{\frac{\sum_{j=1}^m (P_j - \hat{P}_j)^2}{m}} \quad \text{and} \quad \text{Error_Score(RMSE)} = \frac{1}{N} \sum_{i=1}^N \text{RMSE}_i \quad (27)$$

$$\text{MAE}_i = \frac{1}{m} |P_j - \hat{P}_j| \quad \text{and} \quad \text{Error_Score(MAE)} = \frac{1}{N} \sum_{i=1}^N \text{MAE}_i \quad (28)$$

Here, P_j and \hat{P}_j are the real and predicted value of hour j of day i whereas m and N are the number of days and number of hour in a day. In our study, for the year 2023, we have $m = 24$ and $N = 352$. For performance evaluation we computed the RMSE for both daily prices and individual hourly prices. For the daily prices case, the dimensions of the price vectors are 24×1 , whereas, for the individual hour case, the dimensions of the price vectors are 352×1 .

Models	Error_Score(RMSE)		Error_Score(MAE)	
	Daily	Hourly	Daily	Hourly
NAIVE	34.0377	42.6449	28.3159	28.3159
LSTM	26.9965	37.3177	22.4793	22.4793
ARX	57.4466	63.6205	46.1869	46.1869
GPR+SVR	24.1278	30.9610	18.9889	18.9889

Table 1: Performance metrics for different models for year 2023.

We also evaluated the performance of the prediction interval using the average coverage probability

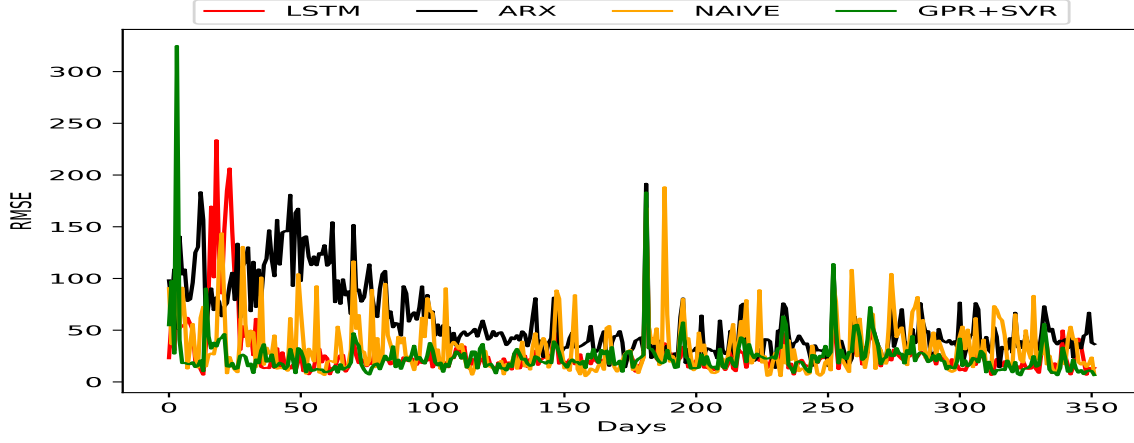


Figure 15: RMSE from 1-Jan-2023 to 17-Dec-2023

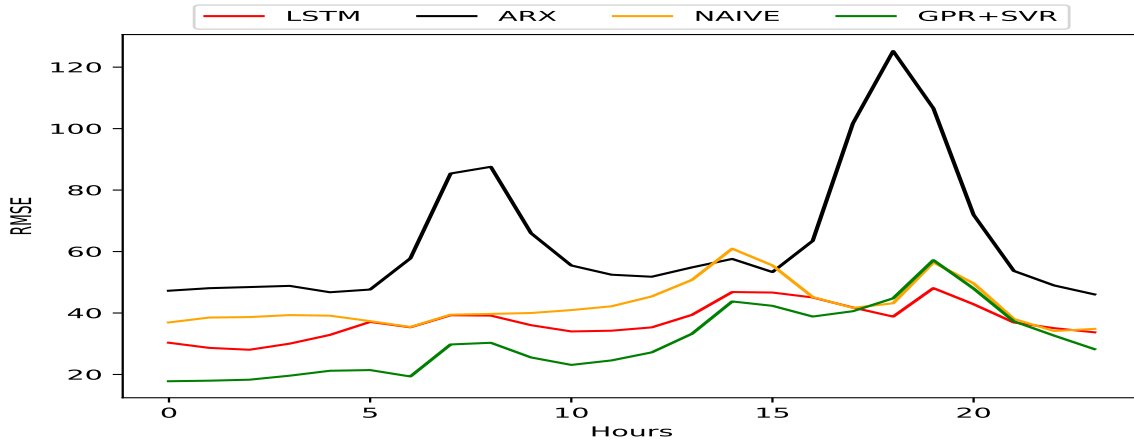


Figure 16: RMSE from 1-Jan-2023 to 17-Dec-2023

as follows:

$$\text{Coverage Probability: } CP = \begin{cases} 1 & \text{if } P_j \in I \\ 0 & \text{if } P_j \notin I \end{cases} \quad \text{and} \quad (29)$$

$$\text{Average Coverage Probability: } ACP_{N,m} = \frac{\frac{1}{N} \sum_{i=1}^N \sum_{j=1}^m CP_j^i}{24} \quad (30)$$

Models	Average Coverage Probability
GPR	0.7632
SVR	0.9056
GPR+SVR	0.8934

Table 2: Prediction Interval Based Performance

In an ideal situation, if the real prices of each hour of every day are within the prediction interval, the $ACP_{N,m}$ is equal to 1. We see from Table (2), that the prediction interval given by SVR is covers most of the real prices on an average. However, SVR itself is not always performing better than GPR on every days of the year, which can be seen from the Figure (13b). This is because we assumed that the model which is performing better on the validation set would also have better coverage. Therefore, we linearly combined the respective lower and upper bounds of prediction interval for GPR and SVR with the weights obtained from the validation set. This study emphasized prediction accuracy more than the prediction interval. If we give more importance to the prediction interval and choose SVR

as our prediction model, then the accuracy of the point predictions will be affected. That said, the coverage of the prediction interval given by the combination of GPR and SVR is not too far from the coverage of prediction interval given by the SVR and is better than that of GPR. It shows only minor difference of 0.0122, which motivates us to choose the combination of GPR and SVR. At the end we present the model performance for the year 2021 and 2022 in table (4) and (3) respectively, which shows that combination of GPR and SVR outperforms the benchmark model we have selected.

Models	Error_Score(RMSE)		Error_Score(MAE)	
	Daily	Hourly	Daily	Hourly
NAIVE	74.7363	92.0359	66.0943	66.0943
LSTM	70.4950	87.9718	62.4768	62.4768
ARX	136.4639	151.5293	117.5713	117.5713
GPR+SVR	53.9284	64.2554	45.5357	45.5357

Table 3: Performance metrics for different models for 2022.

Models	Error_Score(RMSE)		Error_Score(MAE)	
	Daily	Hourly	Daily	Hourly
NAIVE	28.5891	41.0990	24.5976	24.5976
LSTM	20.9651	29.1358	17.6257	17.6257
ARX	40.0091	51.8137	35.3705	35.3705
GPR+SVR	18.9712	24.1544	15.8010	15.8010

Table 4: Performance metrics for different models for 2021.

8 Conclusion and Future Work

We propose a kernel-based model for predicting electricity prices, focusing on the German power market. The choice of kernels is based on the characteristics of the data. The prior knowledge of the behavior of the covariance functions (kernels) used in the model helps interpret the predictions and increases the reliability of the results. Since both GPR and SVR have their own limitations and advantages, combining these two models provides flexibility and robustness. If the performance of one model is suboptimal, a lower weight is assigned to that prediction, while a higher weight is given to the prediction from the other model if it is more accurate, resulting in a better overall prediction. This approach ensures that the best predictions from both GPR and SVR are used, minimizing the risk of unrealistic predictions caused by noise or outliers in the training data.

The issue of extreme values can be addressed by combining the prediction methods that account for such values. However, detecting extreme values and filtering them out for separate modeling adds complexity to the process. In continuation of this work, we plan to apply this approach to investigate the efficiency of this kernel-based predictive model for electricity storage in energy markets. This will aid in grid stabilization and energy arbitrage, as discussed in [56], which currently uses a vector autoregressive model. Further improvements can also be made by combining this model with additional techniques.

References

- [1] C. R. Knittel, M. R. Roberts, An empirical examination of restructured electricity prices, *Energy Economics* 27 (5) (2005) 791–817.
- [2] H. Husin, M. Zaki, et al., A critical review of the integration of renewable energy sources with various technologies, *Protection and control of modern power systems* 6 (1) (2021) 1–18.
- [3] N. Mehmood, N. Arshad, Interval forecasting of hourly electricity spot prices using rolling window based gaussian process regression, in: *2020 2nd International Conference on Smart Power & Internet Energy Systems (SPIES)*, IEEE, 2020, pp. 469–473.
- [4] F. Wang, K. Li, L. Zhou, H. Ren, J. Contreras, M. Shafie-Khah, J. P. Catalão, Daily pattern prediction based classification modeling approach for day-ahead electricity price forecasting, *International Journal of Electrical Power & Energy Systems* 105 (2019) 529–540.
- [5] F. I. for Solar Energy system, Public net electricity generation 2023 in germany: Renewables cover the majority of the electricity consumption for the first time, Press-release (2024) 1–6. URL <https://www.ise.fraunhofer.de/en/press-media/press-releases/2024/public-electricity-generation-2023-renewable-energies-cover-the-majority-of-german-electricity-consumption-for-the-first-time.html>
- [6] C. Cornell, N. T. Dinh, S. A. Pourmousavi, A probabilistic forecast methodology for volatile electricity prices in the australian national electricity market, *International Journal of Forecasting* (2024).
- [7] L. Massidda, F. Bettio, M. Marrocu, Probabilistic day-ahead prediction of pv generation. a comparative analysis of forecasting methodologies and of the factors influencing accuracy, *Solar Energy* 271 (2024) 112422.
- [8] M. A. Zamee, Y. Lee, D. Won, Self-supervised adaptive learning algorithm for multi-horizon electricity price forecasting, *IEEE Access* (2024).
- [9] A. Poggi, L. Di Persio, M. Ehrhardt, Electricity price forecasting via statistical and deep learning approaches: The german case, *AppliedMath* 3 (2) (2023) 316–342.
- [10] X. Xiong, G. Qing, A hybrid day-ahead electricity price forecasting framework based on time series, *Energy* 264 (2023) 126099.
- [11] P. Jiang, Y. Nie, J. Wang, X. Huang, Multivariable short-term electricity price forecasting using artificial intelligence and multi-input multi-output scheme, *Energy Economics* 117 (2023) 106471.
- [12] J. Contreras, R. Espinola, F. J. Nogales, A. J. Conejo, Arima models to predict next-day electricity prices, *IEEE transactions on power systems* 18 (3) (2003) 1014–1020.
- [13] A. J. Conejo, M. A. Plazas, R. Espinola, A. B. Molina, Day-ahead electricity price forecasting using the wavelet transform and arima models, *IEEE transactions on power systems* 20 (2) (2005) 1035–1042.
- [14] O. A. Karabiber, G. Xydis, Electricity price forecasting in the danish day-ahead market using the tbats, ann and arima methods, *Energies* 12 (5) (2019) 928.
- [15] M. Ghayekhloo, R. Azimi, M. Ghofrani, M. Menhaj, E. Shekari, A combination approach based on a novel data clustering method and bayesian recurrent neural network for day-ahead price forecasting of electricity markets, *Electric Power Systems Research* 168 (2019) 184–199.
- [16] R. Zhang, G. Li, Z. Ma, A deep learning based hybrid framework for day-ahead electricity price forecasting, *IEEE Access* 8 (2020) 143423–143436.
- [17] Ç. B. Bozlak, C. F. Yaşar, An optimized deep learning approach for forecasting day-ahead electricity prices, *Electric Power Systems Research* 229 (2024) 110129.
- [18] B. Uniejewski, Regularization for electricity price forecasting, arXiv preprint arXiv:2404.03968 (2024).

- [19] C. O'Connor, J. Collins, S. Prestwich, A. Visentin, Electricity price forecasting in the irish balancing market, *Energy Strategy Reviews* 54 (2024) 101436. doi:<https://doi.org/10.1016/j.esr.2024.101436>.
URL <https://www.sciencedirect.com/science/article/pii/S2211467X24001433>
- [20] J. D. Hamilton, *Time series analysis*, Princeton university press, 2020.
- [21] Y. Guo, Y. Du, P. Wang, X. Tian, Z. Xu, F. Yang, L. Chen, J. Wan, A hybrid forecasting method considering the long-term dependence of day-ahead electricity price series, *Electric Power Systems Research* 235 (2024) 110841.
- [22] C. K. Williams, C. E. Rasmussen, *Gaussian processes for machine learning*, Vol. 2, MIT press Cambridge, MA, 2006.
- [23] A. J. Smola, B. Schölkopf, A tutorial on support vector regression, *Statistics and computing* 14 (2004) 199–222.
- [24] D. Liebl, Modeling and forecasting electricity spot prices: A functional data perspective, *The Annals of Applied Statistics* (2013) 1562–1592.
- [25] R. A. Davis, *Gaussian Process*, John Wiley & Sons, Ltd, 2006, pp. 1–6. arXiv:<https://onlinelibrary.wiley.com/doi/pdf/10.1002/9780470057339.vag002>, doi:<https://doi.org/10.1002/9780470057339.vag002>.
URL <https://onlinelibrary.wiley.com/doi/abs/10.1002/9780470057339.vag002>
- [26] G. A. Pavliotis, *Stochastic processes and applications*, Texts in applied mathematics 60 (2014).
- [27] L. Debnath, D. Bhatta, *Integral transforms and their applications*, Chapman and Hall/CRC, 2016.
- [28] P. Orbanz, Y. W. Teh, Bayesian nonparametric models., *Encyclopedia of machine learning* 1 (2010) 81–89.
- [29] Z. Ghahramani, Bayesian non-parametrics and the probabilistic approach to modelling, *Philosophical Transactions of the Royal Society A: Mathematical, Physical and Engineering Sciences* 371 (1984) (2013) 20110553.
- [30] J. Q. Shi, T. Choi, *Gaussian process regression analysis for functional data*, CRC press, 2011.
- [31] J. Wang, An intuitive tutorial to gaussian processes regression, *Computing in Science & Engineering* (2023).
- [32] Y. L. Tong, *The multivariate normal distribution*, Springer Science & Business Media, 2012.
- [33] A. Wilson, R. Adams, Gaussian process kernels for pattern discovery and extrapolation, in: *International conference on machine learning*, PMLR, 2013, pp. 1067–1075.
- [34] M. G. Genton, Classes of kernels for machine learning: a statistics perspective, *Journal of machine learning research* 2 (Dec) (2001) 299–312.
- [35] N. Ulapane, K. Thiyagarajan, S. Kodagoda, Hyper-parameter initialization for squared exponential kernel-based gaussian process regression, in: *2020 15th IEEE Conference on Industrial Electronics and applications (ICIEA)*, IEEE, 2020, pp. 1154–1159.
- [36] J. Quinonero-Candela, C. E. Rasmussen, A unifying view of sparse approximate gaussian process regression, *The Journal of Machine Learning Research* 6 (2005) 1939–1959.
- [37] X. Du, Y. Cai, Z. Tang, Integrating weather conditions to forecast the electricity price in belgium market: A novel mixed-frequency machine learning algorithm, *Journal of Systems Science and Complexity* (2024) 1–29.
- [38] P. K. Adom, The long-run price sensitivity dynamics of industrial and residential electricity demand: the impact of deregulating electricity prices, *Energy Economics* 62 (2017) 43–60.
- [39] C. Paciorek, M. Schervish, Nonstationary covariance functions for gaussian process regression, *Advances in neural information processing systems* 16 (2003).

- [40] H. Wang, M. J. Bah, M. Hammad, Progress in outlier detection techniques: A survey, *IEEE Access* 7 (2019) 107964–108000. doi:10.1109/ACCESS.2019.2932769.
- [41] K. Choi, J. Yi, C. Park, S. Yoon, Deep learning for anomaly detection in time-series data: Review, analysis, and guidelines, *IEEE Access* 9 (2021) 120043–120065. doi:10.1109/ACCESS.2021.3107975.
- [42] T. Hong, P. Pinson, Y. Wang, R. Weron, D. Yang, H. Zareipour, Energy forecasting: A review and outlook, *IEEE Open Access Journal of Power and Energy* 7 (2020) 376–388. doi:10.1109/OAJPE.2020.3029979.
- [43] V. N. Vapnik, *The nature of statistical learning theory*, Springer-Verlag New York, Inc., 1995.
- [44] B. Schölkopf, A. J. Smola, *Learning with kernels: support vector machines, regularization, optimization, and beyond*, MIT press, 2002.
- [45] N. Cristianini, J. Shawe-Taylor, *Support Vector Machines*, Cambridge University Press, 2000, p. 93–124.
- [46] S. Suthaharan, S. Suthaharan, *Support vector machine, Machine learning models and algorithms for big data classification: thinking with examples for effective learning* (2016) 207–235.
- [47] C. Cortes, V. Vapnik, Support-vector networks, *Machine learning* 20 (1995) 273–297.
- [48] O. Mangasarian, L. 1969. nonlinear programming (1965).
- [49] M. Fontana, G. Zeni, S. Vantini, Conformal prediction: A unified review of theory and new challenges, *Bernoulli* 29 (1) (2023) 1 – 23. doi:10.3150/21-BEJ1447. URL <https://doi.org/10.3150/21-BEJ1447>
- [50] C.-C. Chuang, Z.-J. Lee, Hybrid robust support vector machines for regression with outliers, *Applied Soft Computing* 11 (1) (2011) 64–72.
- [51] L. You, L. Jizhen, Q. Yaxin, A new robust least squares support vector machine for regression with outliers, *Procedia Engineering* 15 (2011) 1355–1360.
- [52] J. Hu, K. Zheng, A novel support vector regression for data set with outliers, *Applied soft computing* 31 (2015) 405–411.
- [53] C.-C. Chuang, J.-T. Jeng, M.-L. Chan, Robust least squares-support vector machines for regression with outliers, in: *2008 IEEE International Conference on Fuzzy Systems (IEEE World Congress on Computational Intelligence)*, IEEE, 2008, pp. 312–317.
- [54] W. Karush, *Minima of functions of several variables with inequalities as side constraints*, M. Sc. Dissertation. Dept. of Mathematics, Univ. of Chicago (1939).
- [55] C.-J. Lin, *A library for support vector machines*, accessed on May (2005).
- [56] S. Schlüter, A. Das, M. Davison, Optimal control of a battery storage on the energy market, arXiv preprint arXiv:2407.20038 (2024).

Appendices

9 Kernel Comparison for SVR

We evaluated the performance of our model using different kernels, namely sigmoid, polynomial, linear, and squared exponential. For each kernel, the grid search method was used to select the best parameters, and the results in Table (5) show that, on average, the model with the squared exponential kernel outperforms the other kernels. Also, our work specifically focused on predicting one day, for which we forecasted the next 48 consecutive hours and used the first 24 hours for validation. We avoided predicting further into the future using the same trained model because the training data for predicting two consecutive days require different estimated parameters, a phenomenon observed in both GPR and SVR. As shown in Tables [6a, 6b, 6c, 6d] and (7), it is clear that the choice of parameters must vary between days, as they are not the same for each prediction.

SVR With	RMSE
Sigmoid Kernel	28.5698
Polynomial Kernel	27.3781
Linear Kernel	26.9071
Squared Exponential Kernel	22.1875

Table 5: Performance of Support Vector Regression with Different Kernels

SN	9-Jan-2023					10-Jan-2023				
	Parameters				Error	Parameters				Error
	C	\hat{c}	d	ϵ		C	\hat{c}	d	ϵ	
1	10	1	3	0.01	84.2953	1	10	1	0.001	88.1374
2	1	1	1	0.01	88.1221	10	1	3	0.1	77.0767
3	0.1	10	3	0.1	117.6192	0.1	10	3	0.1	101.8320
4	10	10	1	0.001	92.2884	10	10	1	0.001	91.0807
5	1	0	1	0.1	88.1157	1	0	1	0.1	88.1160

(a) For Polynomial Kernel

SN	9-Jan-2023					10-Jan-2023				
	Parameters				Error	Parameters				Error
	C	\hat{c}	ϵ	****		C	\hat{c}	ϵ	****	
1	10	0	0.1	82.6621	1	10	0.001	100.3553		
2	1	1	0.01	102.9503	10	10	0.01	75.4209		
3	0.1	10	0.1	117.1683	0.1	10	0.1	117.8115		
4	10	10	0.001	82.6971	10	10	0.001	75.4221		
5	1	0	0.1	102.9690	1	0	0.1	100.3362		

(b) For Squared Exponential Kernel

SN	9-Jan-2023					10-Jan-2023				
	Parameters				Error	Parameters				Error
	C	\hat{c}	ϵ	****		C	\hat{c}	ϵ	****	
1	1	0	0.1	94.4329	1	10	0.001	123.7510		
2	10	10	0.1	123.1427	1	0	0.01	95.3505		
3	0.1	10	0.1	123.1250	0.1	10	0.1	123.7712		
4	10	10	0.001	123.1240	10	10	0.001	123.7507		
5	1	10	0.01	123.1243	1	0	0.1	95.5036		

(c) For Sigmoid Kernel

SN	9-Jan-2023					10-Jan-2023				
	Parameters				Error	Parameters				Error
	C	\hat{c}	ϵ	****		C	\hat{c}	ϵ	****	
1	0.1	0	0.001	88.9259	1	10	0.001	90.3716		
2	1	1	0.01	90.3392	0.1	0	0.1	89.4930		
3	0.1	10	0.01	88.9260	0.1	10	0.01	89.5106		
4	10	10	0.001	93.0460	10	10	0.001	91.7246		
5	1	0	0.1	90.3186	1	0	0.1	90.3028		

(d) For Linear Kernel

Table 6: Estimated Parameters of Support Vector Regression for Prediction of Two Neighbouring Dates

Parameters	9-Jan-2023					
	Covariance Functions					
	SE		Rat.Quad		SE+Rat.Quad	
length scale	$\ell_{se} = 0.7517$	$\ell_{rq} = 0.2067$	$\ell_{se} = 7.5884, \ell_{rq} = 0.2899$			
data variance	$\sigma_{se}^2 = 2.3519$	$\sigma_{rq}^2 = 26.3523$	$\sigma_{se}^2 = 7.5294, \sigma_{rq}^2 = 0.2723$			
noise variance	$\sigma_{nse}^2 = 0.0262$	$\sigma_{nrq}^2 = 0.0086$	$\sigma_n^2 = 0.00796$			
exponent	****	$\alpha_{rq} = 0.0062$	$\alpha_{rq} = 1.1966$			
Parameters	10-Jan-2023					
	Covariance Functions					
	SE		Rat.Quad		SE+Rat.Quad	
length scale	$\ell_{se} = 0.7332$	$\ell_{rq} = 0.2130$	$\ell_{se} = 8.6527, \ell_{rq} = 0.2748$			
data variance	$\sigma_{se}^2 = 2.4466$	$\sigma_{rq}^2 = 25.9149$	$\sigma_{se}^2 = 10.6055, \sigma_{rq}^2 = 0.3044$			
noise variance	$\sigma_{nse}^2 = 0.0246$	$\sigma_{nrq}^2 = 0.0089$	$\sigma_n^2 = 0.00819$			
exponent	****	$\alpha_{rq} = 0.0067$	$\alpha_{rq} = 0.9529$			

Table 7: Estimated Parameters of Covariance functions of Gaussian Process for prediction of price of 9-Jan-2023 and 10-Jan-2023

10 Exploring Periodic Behavior through the Sum of RBF and Rational Quadratic Kernels

Furthermore, in this model, we have not used kernels to capture the periodicity because the combination of the rational quadratic kernel and the squared exponential kernel is capable of tracking the periodicity up to some extent. However, we have tested the same data set for the GPR using the sum of squared exponential and rational quadratic and summing them to the local periodic kernel given by

$$K_{lp}(\mathbf{x}_i, \mathbf{x}_j) = \exp\left(-\frac{2 \sin^2\left(\frac{\pi \|\mathbf{x}_i - \mathbf{x}_j\|}{p}\right)}{\ell_{lp}^2}\right) \cdot \exp\left(-\frac{\|\mathbf{x}_i - \mathbf{x}_j\|^2}{2\sigma_{lp}^2}\right) \quad (31)$$

and in this case the covariance function for the model reads as follows:

$$\begin{aligned}
K'_{\text{GPR}}(\mathbf{x}_i, \mathbf{x}_j) &= K_{se}(\mathbf{x}_i, \mathbf{x}_j) + K_{raq}(\mathbf{x}_i, \mathbf{x}_j) + K_{lp}(\mathbf{x}_i, \mathbf{x}_j) \\
&= \sigma_{se}^2 \exp\left(-\frac{\|\mathbf{x}_i - \mathbf{x}_j\|^2}{2\ell_{se}^2}\right) + \sigma_{raq}^2 \left(1 + \frac{\|\mathbf{x}_i - \mathbf{x}_j\|^2}{2\alpha\ell_{raq}}\right)^{-\alpha} \\
&+ \exp\left(-\frac{2\sin^2\left(\frac{\pi\|\mathbf{x}_i - \mathbf{x}_j\|}{p}\right)}{\ell_{lp}^2}\right) \cdot \exp\left(-\frac{\|\mathbf{x}_i - \mathbf{x}_j\|^2}{2\sigma_{lp}^2}\right)
\end{aligned} \tag{32}$$

Models	RMSE
GPR with K_{GPR}	44.3413
GPR with K'_{GPR}	44.7461

Table 8: Caption

Remark 1. Let $f(x, x')$ be a smooth periodic function defined by:

$$f(x, x') = \sigma^2 \exp\left(-\frac{2\sin^2\left(\frac{\pi|x-x'|}{p}\right)}{\ell^2}\right) \exp\left(-\frac{(x-x')^2}{2\ell^2}\right),$$

where $\sigma > 0$, $\ell > 0$, and $p > 0$. For x and x' in a small interval $\Delta x = x - x'$, the function $f(x)$ can be approximated by the combined kernel:

$$k(x, x') = k_{SE}(x, x') + k_{RQ}(x, x'),$$

where the Radial Basis Function (SE) kernel is:

$$k_{SE}(x, x') = \sigma_{SE}^2 \exp\left(-\frac{(x-x')^2}{2\ell_{SE}^2}\right),$$

and the Rational Quadratic (RQ) kernel is:

$$k_{RQ}(x, x') = \sigma_{RQ}^2 \left(1 + \frac{(x-x')^2}{2\alpha\ell_{RQ}^2}\right)^{-\alpha},$$

with $\sigma_{SE}, \sigma_{RQ} > 0$, $\ell_{SE}, \ell_{RQ} > 0$, and $\alpha > 0$. Given appropriate choices of ℓ_{SE} and ℓ_{RQ} , the kernel $k(x, x')$ approximates the local behavior of $f(x)$ over short intervals.

Proof. Consider the Taylor expansion of $f(x,)$ around x' :

$$f(x) \approx f(x') + f'(x')\Delta x + \frac{1}{2}f''(x')(\Delta x)^2,$$

where $\Delta x = x - x'$.

The function $f(x, x')$ is given by:

$$f(x, x') = \sigma^2 \exp\left(-\frac{2\sin^2\left(\frac{\pi|x|}{p}\right)}{\ell^2}\right) \exp\left(-\frac{x^2}{2\ell^2}\right).$$

For small Δx , we use the approximation:

$$\sin^2\left(\frac{\pi x}{p}\right) \approx \left(\frac{\pi x}{p}\right)^2.$$

Thus:

$$\exp\left(-\frac{2\sin^2\left(\frac{\pi x}{p}\right)}{\ell^2}\right) \approx \exp\left(-\frac{2\pi^2 x^2}{p^2 \ell^2}\right).$$

So:

$$f(x) \approx \sigma^2 \exp\left(-\frac{x^2}{2\ell^2} - \frac{2\pi^2 x^2}{p^2 \ell^2}\right) = \sigma^2 \exp\left(-\frac{x^2 \left(1 + \frac{4\pi^2}{p^2}\right)}{2\ell^2}\right).$$

The squared exponential (SE) Function kernel for small Δx is:

$$k_{\text{SE}}(x, x') \approx \sigma_{\text{SE}}^2 \left(1 - \frac{(\Delta x)^2}{2\ell_{\text{SE}}^2}\right).$$

The Rational Quadratic (RQ) kernel for small Δx is:

$$k_{\text{RQ}}(x, x') \approx \sigma_{\text{RQ}}^2 \left(1 - \frac{(\Delta x)^2}{2\ell_{\text{RQ}}^2}\right).$$

Combining these approximations:

$$k(x, x') = k_{\text{SE}}(x, x') + k_{\text{RQ}}(x, x')$$

$$k(x, x') \approx \sigma_{\text{SE}}^2 \left(1 - \frac{(\Delta x)^2}{2\ell_{\text{SE}}^2}\right) + \sigma_{\text{RQ}}^2 \left(1 - \frac{(\Delta x)^2}{2\ell_{\text{RQ}}^2}\right)$$

$$k(x, x') \approx (\sigma_{\text{SE}}^2 + \sigma_{\text{RQ}}^2) - \left(\frac{\sigma_{\text{SE}}^2}{2\ell_{\text{SE}}^2} + \frac{\sigma_{\text{RQ}}^2}{2\ell_{\text{RQ}}^2}\right) (\Delta x)^2.$$

Thus, the combined kernel $k(x, x')$ approximates the local behavior of $f(x)$ up to the quadratic term in Δx , which captures the local periodicity and smoothness of $f(x)$ over short intervals. By choosing appropriate length scales ℓ_{SE} and ℓ_{RQ} , the combined kernel $k(x, x')$ effectively approximates the function $f(x)$ locally. \square

11 Sum of Gaussian processes

Remark 2. The sum of two independent Gaussian process, $S_1 = \{S_1(t) : t \in T\}$ and $S_2 = \{S_2(t) : t \in T\}$ with respective parameters μ_{S_1}, Σ_{S_1} and μ_{S_2}, Σ_{S_2} is also a Gaussian process with parameter $\mu_{S_1} + \mu_{S_2}, \Sigma_{S_1} + \Sigma_{S_2}$

Proof. Let the sum of two Gaussian process $S_1 = \{S_1(t) : t \in T\}$ and $S_2 = \{S_2(t) : t \in T\}$ be denoted by such that $S = \{S_1(t) + S_2(t) : t \in T\}$. Now we need to show that S is a Gaussian process with mean of S , $\mu_S = \mu_{S_1} + \mu_{S_2}$ and covariance, $\Sigma_S = \Sigma_{S_1} + \Sigma_{S_2}$. It is sufficient to show that any finite collection from S is jointly Gaussian. Let $\tilde{S} = \{S(t_1), S(t_2), \dots, S(t_n)\}$ denotes the finite collection from S such that each $S(t_i) = S_1(t_i) + S_2(t_i)$, $i = 1, \dots, n$, $t_i \in T$. Since each $S_1(t_i)$ and $S_2(t_i)$ are Gaussian random variables, this implies that $S(t_i)$ is also random variable due to which, \tilde{S} forms a Gaussian random vector and the joint distribution of $\{S(t_1), S(t_2), \dots, S(t_n)\}$ is multivariate Gaussian. Hence, S is a Gaussian process.

Next, we show that $\mu_S = \mu_{S_1} + \mu_{S_2}$. We know that

$$\begin{aligned} \mu_S &= \mathbb{E}[S(t)] \\ &= \mathbb{E}[S_1(t) + S_2(t)] \\ &= \mathbb{E}[S_1(t)] + \mathbb{E}[S_2(t)] \\ &= \mu_{S_1} + \mu_{S_2} \end{aligned}$$

Similarly, we showed that $\Sigma_S = \Sigma_{S_1} + \Sigma_{S_2}$ as follows:

$$\begin{aligned}
\Sigma_S(s, t) &= \text{Cov}(S(s), S(t)), \forall s, t \in T \\
&= \text{Cov}(S_1(s) + S_2(s), S_1(t) + S_2(t)) \\
&= \text{Cov}(S_1(s), S_1(t)) + \text{Cov}(S_1(s), S_2(t)) + \text{Cov}(S_2(s), S_1(t)) \\
&\quad + \text{Cov}(S_2(s), S_2(t)) \\
&= \text{Cov}(S_1(s), S_1(t)) + \text{Cov}(S_2(s), S_2(t)) \text{ \{Due to independence,} \\
&\quad \text{the cross covariance is zero\}} \\
&= \Sigma_{S_1}(s, t) + \Sigma_{S_2}(s, t)
\end{aligned}$$

This completes the proof. \square

Let us see the relationship between the posterior mean and covariance functions of the GPR when the data is modelled with two different Gaussian processes with their respective means and covariance functions and when the data is modelled by the sum of two previous covariance functions. For this let us use the data from Section 4. Let $\mathbf{P} = \{P_{\mathbf{t}_1}, \dots, P_{\mathbf{t}_u}\}$ be the given data and we want to do the Gaussian process regression for some $\mathbf{P}^* = \{P_{\mathbf{t}_1^*}, \dots, P_{\mathbf{t}_u^*}\}$ at $\{\mathbf{t}_1^*, \dots, \mathbf{t}_u^*\}$ which are not observable. For this first let us take a Gaussian process say S_1 as defined above with mean function as a zero function and covariance function given by $\Sigma^{(1)}$. Using the expression from equation (3) and (4) we can have the posterior mean, $\mu^{*(1)}$, reads as follows:

$$\mu^{*(1)} = \Sigma_{\mathbf{P}^* \mathbf{P}}^{(1)} \left(\Sigma_{\mathbf{P}}^{(1)} \right)^{-1} \mathbf{P} \quad \text{and} \quad (33)$$

$$\Sigma^{*(1)} = \Sigma_{\mathbf{P}^*}^{(1)} - \Sigma_{\mathbf{P}^* \mathbf{P}}^{(1)} \left(\Sigma_{\mathbf{P}}^{(1)} \right)^{-1} \Sigma_{\mathbf{P} \mathbf{P}^*}^{(1)} \quad (34)$$

Similarly if we do the GPR using a Gaussian process S_2 with zero mean function and covariance function given by $K^{(2)}$ then the posterior mean $\mu^{*(2)}$, reads as follows:

$$\mu^{*(2)} = \Sigma_{\mathbf{P}^* \mathbf{P}}^{(2)} \left(\Sigma_{\mathbf{P}}^{(2)} \right)^{-1} \mathbf{P} \quad \text{and} \quad (35)$$

$$\Sigma^{*(2)} = \Sigma_{\mathbf{P}^*}^{(2)} - \Sigma_{\mathbf{P}^* \mathbf{P}}^{(2)} \left(\Sigma_{\mathbf{P}}^{(2)} \right)^{-1} \Sigma_{\mathbf{P} \mathbf{P}^*}^{(2)} \quad (36)$$

Next, when we do the Gaussian process regression with a Gaussian process say S , which is defined as above with zero mean function and covariance function given by $\Sigma = \Sigma^{(1)} + \Sigma^{(2)}$, then the posterior mean and covariance reads as follows:

$$\mu^* = \Sigma_{\mathbf{P}^* \mathbf{P}} (\Sigma_{\mathbf{P}})^{-1} \mathbf{P} \quad \text{and} \quad (37)$$

$$\Sigma^* = \Sigma_{\mathbf{P}^*} - \Sigma_{\mathbf{P}^* \mathbf{P}} (\Sigma_{\mathbf{P}})^{-1} \Sigma_{\mathbf{P} \mathbf{P}^*} \quad (38)$$

From equation (33) to equation (38), we can rewrite the posterior mean and covariance of the GPR with covariance function as sum of previous two covariance functions in terms of individual posterior.